Bonding Interaction between Group 10 and 11 Metals. Synthesis, Structure and Properties of $[M_3(S_2CNR_2)_6M'_2]^{2+}$ (M = Pt or Pd; M' = Ag or Cu; R = Et, Pr^i, Pr^n, Bu^n or C_6H_{11}) †

Masahiro Ebihara,[a] **Kenji Tokoro,**[a] **Minobu Maeda,**[a] **Masaki Ogami,**[a] **Kaori Imaeda,**[a] **Kenji Sakurai,**[a] **Hideki Masuda**[b] **and Takashi Kawamura** *,[a]

[a] *Department of Chemistry, Faculty of Engineering, Gifu University, Yanagido, Gifu 501-11, Japan*
[b] *Department of Applied Chemistry, Nagoya Institute of Technology, Showa-ku, Nagoya 466, Japan*

The mixed-metal complexes $[M_3(S_2CNR_2)_6M'_2]^{2+}$ (M = Pt or Pd; M' = Ag or Cu; R = Et, Pr^i, Pr^n, Bu^n or C_6H_{11}) have been prepared quantitatively upon mixing stoichiometric amounts of $[M(S_2CNR_2)_2]$ and Ag^+ or $[Cu(MeCN)_4]^+$ in dichloromethane. The structures of nine of them have been determined and are classified into three types: one polymer and two discrete ion structures. Comparison of the structures indicates the existence of a bonding interaction between M and M' that is greater for Pt than Pd and for Ag than Cu. The strong bonding interaction between the Pt and Ag atoms is also supported by the ^{195}Pt–$^{107,109}Ag$ coupling constant of 194 Hz for $[Pt_3(S_2CNBu^n_2)_6Ag_2]^{2+}$.

The chemistry of heterometallic complexes is an interesting field because of their bonding mode, solid-state properties and new catalytic activities. Those complexes derived from univalent Group 11 metals and divalent Group 10 metals have interesting new bonding modes. Uson and co-workers[1] have prepared organometallic complexes with Pt^{II}–Ag^I bonds from Pt^{II} complexes with perhalogenophenyl ligand(s), but the corresponding complexes with Pd–Ag or Pt–Cu bonds have not been examined. Fornies *et al.*[2] reported $[AgM_2(C_6F_5)_4(acac)_2]$ (M = Pt or Pd, acac = acetylacetonate) in which there is a Pt–Ag bond and no Pd–Ag bond, respectively. The formation of mixed-metal complexes with hydride-bridged Pt–M' (M' = Au or Ag) bond(s) from mononuclear Pt^{II} complexes with perhalogenophenyl and hydride ligands has been reported by Venanzi and co-workers.[3,4] An Ni $\cdots$ Ag bonding interaction has been implied in $[Ni(mnt)_2\{Ag(PR_3)_2\}_2]$ (mnt = maleonitriledithiolate, R_3 = Ph_3 or $EtPh_2$) and related compounds.[5]

Dithiocarbamato complexes sometimes act as ligands towards a second metal atom. White and co-workers[6] reported compounds which were prepared from $[M^{III}(S_2CNR_2)_3]$ (M = Co, Cr or Rh; R = alkyl) and CuX (X = Br, I). Their structures were discrete dimers, one-dimensional chains or three-dimensional polymers, where a sulfur atom of a dithiocarbamate ligand bridges between two metal atoms. McCleverty *et al.*[7] prepared $[Fe\{CN(C_6H_4Cl-p)\}_2(S_2CNEt_2)_2\text{-}ZnI_2]$ and Golding *et al.*[8] reported polymeric structures constructed from planar $[Cu^{II}\{S_2C(NC_5H_{10})\}]$ (NC_5H_{10} = piperidyl) and CuX (X = Cl or Br). However, all these complexes do not have a direct metal–metal bond or bonding interaction.

Bis(dialkyldithiocarbamato)-platinum(II) and -palladium(II) complexes usually have square-planar structures and show no indication of additional intermolecular bonding interactions in the crystal.[9] On the other hand, reported Ag^I and Cu^I dithiocarbamato complexes have polymeric,[10] hexameric[11] and tetrameric[12] structures with a dithiocarbamato sulfur atom bridging between the Group 11 cations, implying that a sulfur

atom in a dithiocarbamate ligand has extra valence to co-ordinate a Group 11 cation. Extensive studies on transition-metal dithiocarbamates by Colton and co-workers[13,14] have shown that neutral dithiocarbamate complexes can co-ordinate positively charged metal complexes by sharing the sulfur atoms of the former, *e.g.*, $[Rh_2(S_2CNR_2)_5]^+$[13] and $[Hg_2(S_2CNR_2)_3]^+$ (R = alkyl or CH_2Ph).[14]

During trials to oxidize $[Pt(S_2CNR_2)_2]$ in the expectation of intermolecular association involving the oxidized species, we found that reaction of the Pt complex with Ag^+ resulted in an instantaneous change of optical absorption without precipitation of Ag metal. The new species was shown to be stable from the optical spectra. Isolation and crystal structure analysis revealed that the new species were the hitherto unknown mixed-metal compounds of composition $[Pt_3(S_2CNR_2)_6Ag_2]^{2+}$ constructed from planar bis(dialkyldithiocarbamato)-platinum(II) complexes and silver(I) ions. They gave two types of structures in the crystal, depending on the alkyl group of the dithiocarbamate ligand. One was a two-dimensional cationic polymer[15] and the other a discrete ion.[16] Both types of structure included relatively short Pt–Ag distances that implied the existence of a bonding interaction between the Pt and Ag atoms. To examine the metal–metal interaction of this class of compounds, we decided to explore the formation[17] and crystal structure of the series of complexes $[M_3(S_2CNR_2)_6M'_2]^{2+}$ (M = Pt or Pd; M' = Ag or Cu; R = Et, Pr^n, Pr^i, Bu^n or C_6H_{11}). We report here the results and discuss the bonding interactions between the M and M' atoms. Colton and co-workers[18] have also shown that $[Pt_3(S_2CNR_2)_6Ag_2]^{2+}$ catalyses the exchange of dithiocarbamate ligands on Pt atoms.

Experimental

General.—All solvents were distilled from calcium hydride. Silver tetrafluoroborate and silver perchlorate were dried under vacuum before use. The compounds $[M(S_2CNR_2)_2]$ (M = Pt or Pd) and $[Cu(MeCN)_4]X$ (X = BF_4 or PF_6) were prepared by literature methods.[19,20]

Preparation of $[M_3(S_2CNR_2)_6Ag_2]X_2$.—$[Pt_3(S_2CNPr^i_2)_6\text{-}Ag_2][BF_4]_2$. To a dichloromethane solution (50 cm³) of

---

† *Supplementary data available:* see Instructions for Authors, *J. Chem. Soc., Dalton Trans.*, 1994, Issue 1, pp. xxiii–xxviii.

Non-SI unit employed: eV ≈ 1.60 × 10⁻¹⁹ J.

Table 1 Elemental analyses and melting point data for $[M_3(S_2CNR_2)_6M'_2]X_2$

				Analysis, found (calc. %)				
M	M'	R	X	C	H	N	M.p./°C	Colour
Pt	Ag	Et	ClO_4	19.20 (19.05)	3.15 (3.20)	4.50 (4.45)	244–246[a]	Yellow
Pt	Ag	Pr^i	BF_4	24.70 (24.80)	4.20 (4.15)	4.10 (4.15)	250–280[a]	Yellow
Pt	Ag	Pr^n	BF_4	24.95 (24.80)	4.35 (4.15)	4.20 (4.15)	202–204[a]	Yellow
Pt	Ag	Bu^n	ClO_4	29.35 (29.15)	4.85 (4.90)	3.75 (3.80)	240–243[a]	Yellow
Pt	Ag	Bu^n	BF_4	29.45 (29.45)	4.95 (4.95)	3.85 (3.80)	199–202[a]	Yellow
Pd	Ag	Et	ClO_4	22.20 (22.20)	3.70 (3.70)	5.20 (5.20)	240–241[a]	Yellow
Pd	Ag	Pr^i	BF_4	28.45 (28.55)	4.85 (4.80)	4.75 (4.75)	280–286[a]	Orange
Pd	Ag	Pr^n	ClO_4[b]	27.80 (27.95)	4.65 (4.70)	4.40 (4.45)	183–185	Orange
Pd	Ag	Pr^n	BF_4	28.85 (28.55)	4.70 (4.80)	4.55 (4.75)	199–201[a]	Orange
Pd	Ag	Bu^n	BF_4	33.55 (33.50)	5.80 (5.65)	4.40 (4.35)	189–191[a]	Orange
Pd	Ag	C_6H_{11}	ClO_4	41.50 (41.20)	5.90 (5.85)	3.55 (3.70)	268–272[a]	Orange
Pt	Cu	Et	BF_4	20.15 (20.30)	3.35 (3.40)	4.70 (4.75)	275–276[a]	Yellow
Pt	Cu	Pr^i	BF_4	25.65 (25.95)	4.65 (4.35)	4.05 (4.30)	221–222[a]	Yellow
Pt	Cu	Bu^n	BF_4	30.55 (30.70)	5.20 (5.15)	3.95 (4.00)	223–224[a]	Yellow
Pt	Cu	C_6H_{11}	PF_6	36.60 (36.80)	5.15 (5.20)	3.10 (3.30)	222–224[a]	Yellow
Pd	Cu	Pr^n	BF_4[c]	30.95 (31.00)	5.15 (5.25)	5.00 (4.75)	214–216	Orange
Pd	Cu	Pr^n	PF_6[c]	29.00 (29.05)	4.95 (4.95)	4.50 (4.45)	208–210	Orange
Pd	Cu	C_6H_{11}	BF_4	43.45 (43.30)	6.15 (6.15)	3.60 (3.90)	279–280[a]	Orange

[a] Decomposition. [b] Including the crystalline solvent, $C_2H_4Cl_2$. [c] Including the crystalline solvent, $0.5CH_2Cl_2 \cdot 0.5C_6H_{14}$.

$[Pt(S_2CNPr^i_2)_2]$ (100 mg, 0.18 mmol), $AgBF_4$ (24 mg, 0.12 mmol) in toluene (20 cm³) was added and the mixture stirred for 2 h. After filtration the filtrate was evaporated to dryness to give $[Pt_3(S_2CNPr^i_2)_6Ag_2][BF_4]_2$ as a yellow powder. Yield 100 mg (79%).

The other silver compounds, $[M_3(S_2CNR_2)_6Ag_2]X_2$ (M = Pt; R, X = Et, ClO_4; Pr^n, BF_4; Bu^n, ClO_4; Bu^n, BF_4; M = Pd; R, X = Et, ClO_4; Pr^i, BF_4; Pr^n, ClO_4; Pr^n, BF_4; Bu^n, BF_4; C_6H_{11}, ClO_4), were synthesized similarly. Elemental analyses and melting point data are summarized in Table 1.

Preparation of $[M_3(S_2CNR_2)_6Cu_2]X_2$.—$[Pt_3(S_2CNPr^i_2)_6$-$Cu_2][BF_4]_2$. Under an argon atmosphere a dichloromethane solution (20 cm³) of $[Cu(MeCN)_4]BF_4$ (34 mg, 0.11 mmol) was added to a dichloromethane solution (15 cm³) of $[Pt(S_2CNPr^i_2)_2]$ (91 mg, 0.17 mmol) and the mixture stirred for 1 h. After filtration the filtrate was evaporated to dryness to give $[Pt_3(S_2CNPr^i_2)_6Cu_2][BF_4]_2$ as an orange-yellow powder. Yield 94 mg (87%).

The other copper compounds, $[M_3(S_2CNR_2)_6Cu_2]X_2$ (M = Pt; R, X = Et, BF_4; Bu^n, BF_4; C_6H_{11}, PF_6; M = Pd; R, X = Pr^n, BF_4; Pr^n, PF_6; C_6H_{11}, BF_4), were synthesized similarly. Elemental analyses and melting point data are summarized in Table 1.

Measurements.—The UV/VIS spectra were measured on a Hitachi 150-20 spectrophotometer. Platinum-195 NMR spectra

were recorded on a JEOL GX-400 FT NMR spectrometer with $K_2[PtCl_4]$ in D_2O as external reference. X-Ray photoelectron spectra (XPS) were measured on a Shimadzu ESCA-850 instrument with Mg-Kα radiation. Each sample was loaded as thin plate onto a holder with double-sided tape. The alkyl carbon atoms were used as internal standard (C 1s: 284.0 eV).

X-Ray Crystallography.—All the data were collected on a Rigaku AFC-7R diffractometer with Mo-Kα radiation (λ = 0.710 69 Å). A Rigaku XR-TCS-2-050 temperature controller was used for low-temperature measurements. The cell dimensions were determined by least-squares refinement on diffractometer angles for 25 automatically centred reflections. All the structures were solved and refined using the TEXSAN crystallographic software package on an IRIS Indigo computer. Scattering factors for the neutral atoms were from Cromer and Waber[21] and anomalous dispersion[22] was employed.

$[Pd_3(S_2CNEt_2)_6Ag_2][ClO_4]_2$ **1**. Yellow tabular crystals were grown by slow evaporation of a dichloromethane solution of the compound.

$C_{30}H_{60}Ag_2Cl_2N_6O_8Pd_3S_{12}$, $M = 1623.40$, orthorhombic, $a = 17.270(1)$, $b = 11.264(2)$, $c = 28.562(2)$ Å, $U = 5555.8(9)$ Å³ at 23 ± 1 °C, space group $Pbcn$ (no. 60), $Z = 4$, $D_c = 1.941$ g cm⁻³, $F(000) = 3216$. Crystal dimensions: $0.2 \times 0.1 \times 0.04$ mm, $\mu(Mo$-$K\alpha) = 22.38$ cm⁻¹.

ω Scan modes with scan width = $0.52 + 0.30 \tan \theta$, ω scan

Table 2 Positional parameters for $[Pd_3(S_2CNEt_2)_6Ag_2][ClO_4]_2$ **1**

Atom	x	y	z
Ag(1)	0.347 4(1)	0.947 9(2)	0.801 51(7)
Pd(1)	$\frac{1}{2}$	0.896 7(2)	$\frac{3}{4}$
Pd(2)	0.258 45(9)	0.690 4(2)	0.803 31(5)
Cl(1)	−0.121 3(5)	0.811 7(9)	0.957 3(3)
S(1)	0.502 2(3)	1.021 6(5)	0.814 8(2)
S(2)	0.508 4(4)	0.771 5(5)	0.813 7(2)
S(3)	0.309 2(3)	0.805 1(6)	0.864 2(2)
S(4)	0.363 5(3)	0.598 8(5)	0.768 1(2)
S(5)	0.205 5(3)	0.582 3(5)	0.742 1(2)
S(6)	0.150 7(3)	0.771 9(6)	0.838 5(2)
O(1)	−0.085(2)	0.787(2)	0.915 7(8)
O(2)	−0.194(2)	0.790(3)	0.956(1)
O(3)	−0.114(2)	0.933(2)	0.961 0(9)
O(4)	−0.092(1)	0.752(3)	0.993 0(8)
N(1)	0.528 1(8)	0.897(2)	0.894 0(5)
N(2)	0.191(1)	0.899(2)	0.914 0(7)
N(3)	0.317(1)	0.471(1)	0.692 1(6)
C(11)	0.515(1)	0.897(2)	0.848 5(7)
C(12)	0.533(1)	1.011(2)	0.920 9(7)
C(13)	0.456(1)	1.044(2)	0.940 7(7)
C(14)	0.532(1)	0.782(2)	0.920 7(8)
C(15)	0.611(2)	0.746(3)	0.929(1)
C(21)	0.212(1)	0.838(2)	0.876 9(8)
C(22)	0.252(2)	0.929(3)	0.961(1)
C(23)	0.256(2)	1.041(4)	0.944(1)
C(24)	0.103(1)	0.907(2)	0.927 0(8)
C(25)	0.073(1)	1.008(2)	0.902(1)
C(31)	0.300(1)	0.537(2)	0.729 3(6)
C(32)	0.255(1)	0.423(2)	0.661 2(7)
C(33)	0.238(1)	0.511(2)	0.624 6(8)
C(34)	0.405(1)	0.448(2)	0.680 8(8)
C(35)	0.426(1)	0.332(2)	0.700(1)

speed 32° min^{-1}, graphite-monochromated Mo-Kα radiation at 23 ± 1 °C; 7069 reflections measured (1.5 $\leq \theta \leq$ 27.5°, h,k,l), giving 2284 with $I > 2\sigma(I)$. Absorption correction (DIFABS[23]) with transmission factors 0.702–1.135. No significant decay was observed.

Direct methods SHELX 86[24] (Pd and Ag atoms) followed by normal heavy-atom procedures. Full-matrix least-squares refinement with all atoms anisotropic except some ethyl carbon atoms, which were refined with isotropic thermal parameters. The weighting scheme was $w = [\sigma^2(F_o) + (0.007)^2(F_o)^2/4]^{-1}$. Final R and R' values were 0.078, 0.067. Final atomic coordinates are listed in Table 2.

$[Pd_3(S_2CNPr^i_2)_6Ag_2][BF_4]_2 \cdot 3CH_2Cl_2$ **2**. Orange prismatic crystals were obtained by slow diffusion of n-hexane into a dichloromethane solution of the compound. Since they lost crystalline dichloromethane quickly, a crystal was put under a cold nitrogen stream (-10 °C) immediately after mounting on a glass fibre.

$C_{45}H_{90}Ag_2B_2Cl_6F_8N_6Pd_3S_{12}$, $M = 2021.23$, monoclinic, $a = 11.784(3)$, $b = 30.516(3)$, $c = 21.674(3)$ Å, $\beta = 94.11(2)°$, $U = 7774(1)$ Å^3 at $-150 ± 1$ °C, space group $P2_1/c$ (no. 14), $Z = 4$, $D_c = 1.727$ g cm^{-3}, $F(000) = 4040$. Crystal dimensions: 0.3 × 0.2 × 0.2 mm, μ(Mo-Kα) = 17.57 cm^{-1}.

ω Scan modes with scan width = 1.42 + 0.30 tan θ, ω scan speed 32° min^{-1}, graphite-monochromated Mo-Kα radiation at $-150 ± 2$ °C; 19 083 reflections measured (1.5 $\leq \theta \leq$ 27.5°, $h,k,\pm l$), 18 187 unique (merging $R = 0.029$), giving 11 209 with $I > 3\sigma(I)$. Correction for absorption was not applied. No significant decay was observed.

Direct methods SHELX 86[24] (Pd and Ag atoms) followed by normal heavy-atom procedures. A BF$_4^-$ group was disordered and refined in two positions by using a rigid model.[25] The F(21) atom was not disordered and B(2), F(22), F(23) and F(24) made one group (58%) and B(3), F(25), F(26) and F(27)

made the other (42%). Full-matrix least-squares refinement with anisotropic thermal parameters for the other non-hydrogen atoms. The weighting scheme was $w = [\sigma^2(F_o) + (0.003)^2(F_o)^2/4]^{-1}$. Final R and R' values were 0.061, 0.052. Final atomic coordinates are listed in Table 3.

$[Pt_3(S_2CNEt_2)_6Cu_2][BF_4]_2 \cdot C_2H_4Cl_2$ **3**. Yellow prismatic crystals were obtained by slow diffusion of n-hexane into a 1,2-dichloroethane solution of the compound.

$C_{32}H_{64}B_2Cl_2Cu_2F_8N_6Pt_3S_{12}$, $M = 1874.49$, monoclinic, $a = 11.114(3)$, $b = 29.074(4)$, $c = 18.842(4)$ Å, $\beta = 95.00(3)°$, $U = 6065(2)$ Å^3 at $23 ± 1$ °C, space group $P2_1/c$ (no. 14), $Z = 4$, $D_c = 2.053$ g cm^{-3}, $F(000) = 3592$. Crystal dimensions: 0.2 × 0.1 × 0.1 mm, μ(Mo-Kα) = 81.14 cm^{-1}.

ω Scan modes with scan width = 0.73 + 0.20 tan θ, ω scan speed 16° min^{-1}, graphite-monochromated Mo-Kα radiation at $23 ± 1$ °C; 14 932 reflections measured (1.5 $\leq \theta \leq$ 27.5°, $h,k,\pm l$), 14 219 unique [merging $R = 0.050$ after empirical absorption correction with the ψ-scan method[26] (min., max. transmission factors = 0.668, 1.000)], giving 5412 with $I > 3\sigma(I)$. No significant decay was observed.

Direct methods SHELX 86[24] (Pt atoms) followed by normal heavy-atom procedures. Full-matrix least-squares refinement with the BF$_4^-$ ions as rigid groups, the ethyl carbon atoms isotropic and all other non-hydrogen atoms anisotropic. The weighting scheme was $w = [\sigma^2(F_o) + (0.007)^2(F_o)^2/4]^{-1}$. Final R and R' values were 0.055, 0.051. Final atomic coordinates are listed in Table 4.

$[Pt_3(S_2CNPr^i_2)_6Cu_2][BF_4]_2 \cdot 2CH_2Cl_2$ **4**. Yellow prismatic crystals were obtained by slow diffusion of n-hexane into a dichloromethane solution of the compound. A crystal was treated similarly to **2** because of facile loss of crystalline dichloromethane.

$C_{44}H_{88}B_2Cl_4Cu_2F_8N_6Pt_3S_{12}$, $M = 2113.72$, monoclinic, $a = 13.253(2)$, $b = 28.503(4)$, $c = 19.438(2)$ Å, $\beta = 94.16(1)°$, $U = 7323(1)$ Å^3 at $-150 ± 1$ °C, space group $P2_1/c$ (no. 14), $Z = 4$, $D_c = 1.917$ g cm^{-3}, $F(000) = 4112$. Crystal dimensions: 0.45 × 0.3 × 0.2 mm, μ(Mo-Kα) = 68.02 cm^{-1}.

ω Scan modes with scan width = 1.21 + 0.30 tan θ, ω scan speed 32° min^{-1}, graphite-monochromated Mo-Kα radiation at $-150 ± 2$ °C; 17 861 reflections measured (1.5 $\leq \theta \leq$ 27.5°, $h,k,\pm l$), 17 139 unique [merging $R = 0.035$ after an empirical absorption correction DIFABS[23] (min., max. transmission factors = 0.902, 1.101)], giving 10 780 with $I > 3\sigma(I)$. No significant decay was observed.

Direct methods SHELX 86[24] (Pt and Cu atoms) followed by normal heavy-atom procedures. Full-matrix least-squares refinement with all the non-hydrogen atoms anisotropic. The weighting scheme was $w = [\sigma^2(F_o) + (0.007)^2(F_o)^2/4]^{-1}$. Final R and R' values were 0.046, 0.046. Final atomic coordinates are listed in Table 5.

$[Pt_3\{S_2CN(C_6H_{11})_2\}_6Cu_2][PF_6]_2 \cdot 2.73CH_2Cl_2$ **5**. Yellow prismatic crystals were grown by slow diffusion of n-hexane into a dichloromethane solution of the compound. The crystal contained crystalline solvent molecules which were lost upon exposure to the open air at room temperature.

$C_{80.73}H_{137.46}Cl_{5.46}Cu_2F_{12}N_6P_2Pt_3S_{12}$, $M = 2772.79$, monoclinic, $a = 27.508(6)$, $b = 12.324(4)$, $c = 33.364(8)$ Å, $\beta = 112.65(2)°$, $U = 10 438(8)$ Å^3 at $-150 ± 1$ °C, space group $P2_1/a$ (no. 14), $Z = 4$. Crystal dimensions: 0.3 × 0.25 × 0.2 mm, μ(Mo-Kα) = 49.17 cm^{-1}.

ω Scan modes with scan width = 1.05 + 0.30 tan θ, ω scan speed 32° min^{-1}, graphite-monochromated Mo-Kα radiation at $-150 ± 2$ °C. 10 624 Reflections measured (1.5 $\leq \theta \leq$ 20.0°, $h,k,\pm l$), 10 346 unique [merging $R = 0.043$ after DIFABS[23] absorption correction (min., max. transmission factors = 0.788, 1.173)], giving 6751 with $I > 3\sigma(I)$. No decay was detected.

Direct methods SHELX 86[24] (Pt and Cu atoms) followed by normal heavy-atom procedures. Full-matrix least-squares refinement with the cyclohexyl carbon atoms isotropic and all other non-hydrogen atoms anisotropic for the complex and the counter ions. The crystal had three types of crystalline

Table 3 Positional parameters for $[Pd_3(S_2CNPr^i_2)_6Ag_2][BF_4]_2 \cdot 3CH_2Cl_2$ **2**

Atom	x	y	z	Atom	x	y	z
Ag(1)	0.164 77(7)	0.798 30(3)	0.408 80(4)	C(115)	0.214(1)	0.944 0(3)	0.406 5(6)
Ag(2)	0.298 90(7)	0.713 79(3)	0.383 74(4)	C(116)	0.392(1)	0.958 7(4)	0.478 9(5)
Pd(1)	0.394 99(7)	0.785 67(3)	0.466 28(4)	C(121)	0.372(1)	0.667 3(8)	0.630 0(8)
Pd(2)	0.015 54(7)	0.721 74(3)	0.415 58(4)	C(122)	0.443(1)	0.675 3(5)	0.683 6(7)
Pd(3)	0.222 39(7)	0.749 87(3)	0.263 53(4)	C(123)	0.255(1)	0.648 6(4)	0.622 0(6)
Cl(1)	−0.010 9(3)	0.450 5(1)	0.436 4(1)	C(124)	0.494(1)	0.630 6(5)	0.541(1)
Cl(2)	0.109 8(3)	0.388 3(1)	0.519 6(2)	C(125)	0.619(1)	0.641 5(5)	0.562 6(6)
Cl(3)	0.265 6(4)	0.530 2(1)	0.628 8(3)	C(126)	0.448(2)	0.595 3(9)	0.522(1)
Cl(4)	0.360 1(4)	0.448 8(2)	0.593 7(2)	C(211)	−0.083(1)	0.842 5(4)	0.568 7(5)
Cl(5)	0.231 7(5)	0.548 3(2)	0.113 7(3)	C(212)	0.020(1)	0.871 5(4)	0.552 7(5)
Cl(6)	0.129 4(5)	0.477 9(2)	0.037 4(3)	C(213)	−0.055(1)	0.809 9(4)	0.621 9(5)
S(11)	0.316 3(2)	0.854 65(9)	0.471 5(1)	C(214)	−0.263 6(8)	0.829 0(4)	0.494 1(5)
S(12)	0.463 1(2)	0.823 57(9)	0.382 9(1)	C(215)	−0.281(1)	0.878 7(4)	0.481 7(6)
S(13)	0.477 8(2)	0.716 3(1)	0.465 9(1)	C(216)	−0.332 1(9)	0.811 5(4)	0.547 5(5)
S(14)	0.330 1(2)	0.751 1(1)	0.552 0(1)	C(221)	0.024(1)	0.580 5(4)	0.294 0(5)
S(21)	0.053 6(2)	0.771 36(9)	0.497 0(1)	C(222)	0.088(1)	0.570 7(5)	0.236 2(6)
S(22)	−0.138 2(2)	0.769 6(1)	0.407 7(1)	C(223)	−0.047(1)	0.544 5(4)	0.320 7(6)
S(23)	−0.031 0(2)	0.672 81(9)	0.336 6(1)	C(224)	0.200(1)	0.572 1(4)	0.370 5(5)
S(24)	0.153 7(2)	0.667 50(8)	0.428 2(1)	C(225)	0.182(1)	0.554 7(4)	0.434 4(5)
S(31)	0.191 9(2)	0.820 30(8)	0.300 8(1)	C(226)	0.317(1)	0.592 3(4)	0.360 4(6)
S(32)	0.037 7(3)	0.765 8(1)	0.229 3(1)	C(311)	0.011(1)	0.891 7(4)	0.292 8(5)
S(33)	0.249 7(3)	0.681 3(1)	0.220 9(1)	C(312)	0.027(1)	0.929 1(3)	0.247 5(6)
S(34)	0.412 1(2)	0.733 28(9)	0.290 9(1)	C(313)	−0.088(1)	0.899 4(5)	0.336 7(7)
F(11)	0.239 0(6)	0.470 4(2)	0.802 6(3)	C(314)	−0.128(1)	0.849 5(4)	0.214 6(6)
F(12)	0.128 8(6)	0.448 1(2)	0.877 5(4)	C(315)	−0.212(1)	0.814 8(4)	0.236 3(6)
F(13)	0.318 8(6)	0.446 1(2)	0.892 3(3)	C(316)	−0.094(1)	0.843 7(4)	0.145 6(5)
F(14)	0.228 1(6)	0.398 7(2)	0.826 0(3)	C(321)	0.597(1)	0.662 9(4)	0.255 6(7)
F(21)	0.352 5(7)	0.417 9(3)	0.298 0(4)	C(322)	0.621(1)	0.660 8(5)	0.325 8(6)
N(11)	0.401 6(7)	0.909 3(3)	0.385 8(4)	C(323)	0.645(1)	0.703 4(4)	0.226 1(7)
N(12)	0.425 9(8)	0.668 5(4)	0.567 0(6)	C(324)	0.435(1)	0.615 8(4)	0.197 7(5)
N(21)	−0.137 9(7)	0.820 1(3)	0.510 3(4)	C(325)	0.470(1)	0.623 6(4)	0.131 0(5)
N(22)	0.103 4(8)	0.600 5(3)	0.345 5(4)	C(326)	0.490(1)	0.573 9(3)	0.226 2(5)
N(31)	−0.015 9(7)	0.849 6(3)	0.256 5(4)	C(401)	0.120(1)	0.440 2(4)	0.480 8(6)
N(32)	0.471 6(9)	0.657 0(3)	0.236 3(4)	C(402)	0.354(1)	0.487 2(4)	0.654 4(7)
C(11)	0.395 7(9)	0.869 1(3)	0.409 5(5)	C(403)	0.116(2)	0.513 2(6)	0.101(1)
C(12)	0.411 2(8)	0.705 6(4)	0.534 3(5)	B(1)	0.230(1)	0.440 9(4)	0.850 8(7)
C(21)	−0.081 0(8)	0.792 7(3)	0.476 3(4)	B(21)[a]	0.311 7(8)	0.455 7(3)	0.310 7(5)
C(22)	0.080 4(9)	0.640 0(3)	0.365 4(5)	F(22)[a]	0.242(1)	0.449 9(6)	0.357 5(6)
C(31)	0.055 8(9)	0.817 4(3)	0.261 7(5)	F(23)[a]	0.254(1)	0.477 6(4)	0.263 5(5)
C(32)	0.391(1)	0.685 0(3)	0.248 3(5)	F(24)[a]	0.404 3(8)	0.479 5(5)	0.331 5(6)
C(111)	0.470(1)	0.917 5(3)	0.330 5(5)	B(22)[b]	0.332(1)	0.456 5(4)	0.335 5(6)
C(112)	0.567(1)	0.950 3(4)	0.349 8(6)	F(25)[b]	0.360(1)	0.491 7(5)	0.301 1(6)
C(113)	0.392(1)	0.932 1(4)	0.275 6(5)	F(26)[b]	0.387(1)	0.459 2(7)	0.392 6(7)
C(114)	0.344(1)	0.949 0(3)	0.413 1(6)	F(27)[b]	0.218(1)	0.456 3(6)	0.340 9(8)

[a] 58% occupancy. [b] 42% occupancy.

dichloromethane molecules. Two were disordered and one was refined with 0.73 occupancy. The weighting scheme was $w = [\sigma^2(F_o) + (0.007)^2(F_o)^2/4]^{-1}$. Final R and R' values were 0.053, 0.054. Final atomic coordinates are listed in Table 6.

$[Pd_3(S_2CNPr^n_2)_6Cu_2][PF_6]_2 \cdot 0.5CH_2Cl_2 \cdot 0.5C_6H_{14}$ **6**. Orange prismatic crystals were grown by slow diffusion of n-hexane into a dichloromethane solution of the compound. Preliminary structure determination at 23 °C indicated the existence of crystalline solvent. The measured density of 1.63 g cm^{-3} agreed well with both of the calculated densities of 1.621 g cm^{-3} for $[Pd_3(S_2CNPr^n_2)_6Cu_2][PF_6]_2 \cdot CH_2Cl_2$ and of 1.620 g cm^{-3} for $[Pd_3(S_2CNPr^n_2)_6Cu_2][PF_6]_2 \cdot C_6H_{14}$. Elemental analysis [C, 29.00; H, 4.95; N, 4.50%] was not consistent with either. We assumed a formula $[Pd_3(S_2CNPr^n_2)_6Cu_2][PF_6]_2 \cdot nCH_2Cl_2 \cdot (1 - n)C_6H_{14}$ and $n = 0.5$ gave the calculated values [C, 29.05; H, 4.95; N, 4.45%], consistent with the experimental ones (Table 1). Proton NMR data also supported this formula.

$C_{45.5}H_{92}ClCu_2F_{12}N_6P_2Pd_3S_{12}$, $M = 1879.79$, monoclinic, $a = 20.606(2)$, $b = 30.240(4)$, $c = 12.003(3)$ Å, $\beta = 90.02(1)°$, $U = 7479(1)$ Å^3 at -72 ± 1 °C, space group $P2_1/n$ (no. 14),

$Z = 4$, $D_c = 1.669$ g cm^{-3}, $F(000) = 3800$. Crystal dimensions: $0.3 \times 0.25 \times 0.1$ mm, $\mu(Mo-K\alpha) = 17.46$ cm^{-1}.

ω Scan modes with scan width $= 1.73 + 0.30 \tan \theta$, ω scan speed 32° min^{-1}, graphite-monochromated Mo-Kα radiation at -72 ± 2 °C; 17 985 reflections measured ($1.5 \leqslant \theta \leqslant 27.5°$, $h,k,\pm l$), 17 515 unique (merging $R = 0.048$), giving 6086 with $I > 3\sigma(I)$. No significant decay was observed.

Direct methods MITHRIL[27] gave the positions of the Pd and Cu atoms. The whole structure of $[Pd_3(S_2CNPr^n_2)_6Cu_2][PF_6]_2$ was expanded by a Fourier difference method. Full-matrix least-squares refinement with all non-hydrogen atoms anisotropic except some alkyl carbons atoms, which were refined isotropically. The weighting scheme was $w = [\sigma^2(F_o) + (0.002)^2(F_o)^2/4]^{-1}$. Peaks from a final Fourier difference map could not be refined because of disorder of the crystalline dichloromethane and hexane. The crystalline solvent molecules were not included in the refinements. Final R and R' values were 0.079, 0.092. Final atomic coordinates are listed in Table 7.

$[Pt_3(S_2CNPr^i_2)_6Ag_2][BF_4]_2$ **7**. Yellow crystals were obtained by slow evaporation from a dichloromethane solution of the compound.

Table 4 Positional parameters for $[Pt_3(S_2CNEt_2)_6Cu_2][BF_4]_2 \cdot C_2H_4Cl_2$ **3**

Atom	x	y	z	Atom	x	y	z
Pt(1)	0.740 64(8)	0.252 20(3)	0.063 34(4)	C(112)	0.504(3)	0.419 4(9)	−0.004(1)
Pt(2)	0.569 37(8)	0.234 91(3)	0.280 41(4)	C(113)	0.329(3)	0.334 0(9)	0.026(1)
Pt(3)	0.901 70(8)	0.269 37(3)	0.298 14(4)	C(114)	0.272(3)	0.323(1)	0.096(2)
Cu(1)	0.736 2(3)	0.306 98(9)	0.189 1(1)	C(121)	1.161(3)	0.168(1)	0.081(2)
Cu(2)	0.735 5(3)	0.198 1(1)	0.182 8(1)	C(122)	1.190(3)	0.180(1)	0.016(2)
Cl(1)	0.227 8(9)	0.180 8(4)	0.322 2(7)	C(123)	0.981(2)	0.106 7(7)	0.035(1)
Cl(2)	0.249 9(7)	0.324 9(3)	0.304 8(5)	C(124)	0.969(2)	0.078 9(8)	0.104(1)
S(11)	0.703 1(6)	0.331 1(2)	0.066 0(3)	C(211)	0.515(3)	0.413(1)	0.274(2)
S(12)	0.532 2(6)	0.259 4(2)	0.043 9(3)	C(212)	0.627(4)	0.422(1)	0.259(2)
S(13)	0.775 1(6)	0.173 6(2)	0.055 9(3)	C(213)	0.587(2)	0.389 5(7)	0.412(1)
S(14)	0.949 2(5)	0.244 0(2)	0.077 6(3)	C(214)	0.470(3)	0.389 6(8)	0.442(1)
S(21)	0.553 1(5)	0.307 8(2)	0.229 5(5)	C(221)	0.499(2)	0.077 5(7)	0.164(1)
S(22)	0.593 1(5)	0.285 0(2)	0.376 2(3)	C(222)	0.618(2)	0.059 8(8)	0.140(1)
S(23)	0.571 5(6)	0.163 0(2)	0.335 2(3)	C(223)	0.518(2)	0.061 4(8)	0.300(1)
S(24)	0.535 9(5)	0.182 5(2)	0.186 0(3)	C(224)	0.391(3)	0.054 2(9)	0.310(1)
S(31)	0.938 8(5)	0.323 0(2)	0.209 7(3)	C(311)	1.003(2)	0.425 2(7)	0.198(1)
S(32)	0.903 1(6)	0.340 1(2)	0.355 2(3)	C(312)	0.887(2)	0.444 9(8)	0.159(1)
S(33)	0.878 2(6)	0.218 7(2)	0.390 0(3)	C(313)	0.978(2)	0.440 4(8)	0.331(1)
S(34)	0.915 2(5)	0.196 5(2)	0.247 3(3)	C(314)	1.105(2)	0.443 1(8)	0.362(1)
N(11)	0.462(2)	0.349 2(6)	0.044 7(9)	C(321)	0.901(2)	0.093 9(7)	0.295(1)
N(12)	1.015(2)	0.154 8(6)	0.055(1)	C(322)	1.018(3)	0.073 1(9)	0.301(1)
N(21)	0.571(2)	0.375 3(5)	0.334(1)	C(323)	0.875(2)	0.117 0(7)	0.426(1)
N(22)	0.520(2)	0.094 6(6)	0.239(1)	C(324)	0.995(2)	0.119 6(8)	0.473(1)
N(31)	0.970(2)	0.407 9(5)	0.267(1)	B(1)	0.255(1)	0.013 6(3)	0.069 3(5)
N(32)	0.890(2)	0.130 7(5)	0.348 9(9)	F(1)	0.246(1)	0.057 1(4)	0.043 2(8)
C(1)	0.242(3)	0.251(2)	0.348(2)	F(2)	0.168(1)	−0.013 3(5)	0.035 3(9)
C(2)	0.233(3)	0.255(1)	0.279(2)	F(3)	0.366(1)	−0.003 7(6)	0.059(1)
C(11)	0.551(2)	0.317 7(8)	0.050(1)	F(4)	0.241(2)	0.014 1(6)	0.140 3(5)
C(12)	0.926(2)	0.186 1(7)	0.061(1)	B(2)	0.243(1)	0.018 4(5)	0.611 9(8)
C(21)	0.571(2)	0.330 3(7)	0.320(1)	F(5)	0.225(2)	0.063 1(6)	0.593(1)
C(22)	0.540(2)	0.138 3(7)	0.252(1)	F(6)	0.150(2)	−0.007 6(9)	0.582(2)
C(31)	0.942(2)	0.365 5(6)	0.278(1)	F(7)	0.348(2)	0.003 3(9)	0.589(1)
C(32)	0.894(2)	0.173 0(7)	0.333(1)	F(8)	0.247(3)	0.015(1)	0.684 1(8)
C(111)	0.497(2)	0.397 7(8)	0.062(1)				

$C_{42}H_{84}Ag_2B_2F_8N_6Pt_3S_{12}$, $M = 2032.50$, orthorhombic, $a = 11.368(3), b = 29.700(2), c = 20.258(3)$ Å, $U = 6840(1)$ Å^3 at $-150 \pm 1\,°C$, space group $Pccn$ (no. 56), $Z = 4$, $D_c = 1.974$ g cm^{-3}, $F(000) = 3920$. Crystal dimensions: $0.2 \times 0.15 \times 0.1$ mm, $\mu(Mo-K\alpha) = 70.72$ cm^{-1}.

ω Scan modes with scan width $= 1.05 + 0.30$ tan θ, ω scan speed $32°$ min^{-1}, graphite-monochromated Mo-Kα radiation at $-150 \pm 2\,°C$; 8653 reflections measured ($1.5 \leqslant \theta \leqslant 27.5°$, h,k,l), giving 4560 with $I > 3\sigma(I)$. A DIFABS^{23} empirical absorption correction (min., max. transmission factors $= 0.906$, 1.089) was applied. No significant decay was detected.

The structure was solved by using the structure obtained at 23 °C and reported earlier.[16] Full-matrix least-squares refinement with anisotropic refinement for all non-hydrogen atoms. The weighting scheme employed was $w = [\sigma^2(F_o) + (0.011)^2(F_o)^2/4]^{-1}$. Final R and R' values were 0.041, 0.041. Final atomic coordinates are listed in Table 8.

Additional material available from the Cambridge Crystallographic Data Centre comprises thermal parameters and remaining bond lengths and angles.

Results and Discussion

Synthesis.—The reaction between $[M(S_2CNR_2)_2]$ (M = Pt or Pd) and Ag or Cu was monitored by UV/VIS absorption during successive additions of a concentrated solution of Ag^I or Cu^I ion to a dilute solution of $[M(S_2CNR_2)_2]$. The change in absorption during the addition of AgBF$_4$ to a solution of $[Pt(S_2CNPr^i_2)_2]$ is shown in Fig. 1, which shows that the reaction takes place in two steps. The first step is complete at the mixing mole ratio of 3:2 (Pt:Ag) and the second one at 1:2. The sharpness of the change in the absorbance dependence on the

mixing ratio indicates that the 3:2 complex does not dissociate appreciably in CH$_2$Cl$_2$. Until the complete formation of the 3:2 product, two isosbestic points were observed at 340 and 378 nm. The reaction product of the first step was $[Pt_3(S_2CNPr^i_2)_6Ag_2]^{2+}$ which has an absorption peak at 322 nm. Two isosbestic points were observed at 317 and 365 nm during the formation of $[Pt(S_2CNPr^i_2)_2Ag_2]^{2+}$. The reactions between the other $[Pt(S_2CNR_2)_2]$ complexes and Ag^I ion in dichloromethane, chloroform or 1,2-dichloroethane gave similar patterns. The palladium dithiocarbamates also gave $[Pd_3(S_2CNR_2)_6Ag_2]^{2+}$ and $[Pd(S_2CNR_2)_2Ag_2]^{2+}$ when mixed with Ag$^+$ salts in halogenated hydrocarbons.

The compounds $[M_3(S_2CNR_2)_6Ag_2]X_2$ (M = Pt or Pd; R = Et, Pr^n, Pr^i, Bu^n or C$_6$H$_{11}$; X = ClO$_4$ or BF$_4$) were isolated by evaporation of a dichloromethane solution of a stoichiometric mixture of $[M(S_2CNR_2)_2]$ and AgX. All the complexes dissolved readily in dichloromethane or 1,2-dichloroethane except the diethyldithiocarbamato derivatives of the Pt–Ag and Pd–Ag mixed metal compounds, which decreased in solubility once they were precipitated. The 1:2 products, $[M(S_2CNR_2)_2Ag_2]X_2$, were obtained as orange powders upon mixing stoichiometric amounts of solutions of $[M(S_2CNR_2)_2]$ and AgX. Once the 1:2 products were precipitated, they did not re-dissolve in the usual organic solvents.

Absorption spectra observed during the successive addition of a dichloromethane solution of $[Cu(MeCN)_4]BF_4$ to a dichloromethane solution of $[Pt(S_2CNPr^i_2)_2]$ are shown in Fig. 2. It shows the formation of only $[Pt_3(S_2CNPr^i_2)_6Cu_2]^{2+}$. The 3:2 species was also formed in chloroform or 1,2-dichloroethane. Reaction of the palladium dithiocarbamates and $[Cu(MeCN)_4]^+$ gave only $[Pd_3(S_2CNR_2)_6Cu_2]^{2+}$ as in the

case of the Pt–Cu system. All the mixed-metal compounds derived from copper were stable to air even in solution.

Structure.—The crystal structures of three Pt–Ag, one Pd–Cu, two Pd–Ag and three Pt–Cu compounds have been determined. They can be classified into three types based on their crystal structures. Type I compounds consist of cationic

polymer and counter anions, and $[M_3(S_2CNEt_2)_6Ag_2][ClO_4]_2$ [M = Pt **8**[15] or Pd **1**] belong to this type. Fig. 3(*a*) shows a representative structure of the compounds which are classified as type II. This type has a discrete cation such as $[Pt_3(S_2CNPr^i_2)_6Ag_2]^{2+}$ or $[Pt_3(S_2CNBu^n_2)_6Ag_2]^{2+}$ which has a pseudo-three-fold axis through the two Ag atoms.[16] Type III compounds contain a discrete cation which does not have the three-fold axis. [Fig. 3(*b*) and 3(*c*)]. The two type III structures differ from each other in the number of
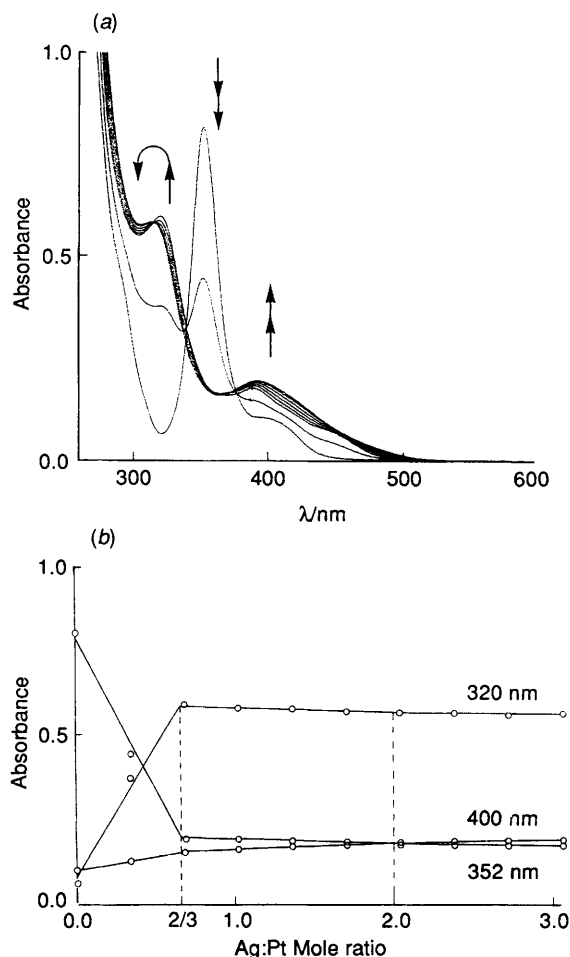

Fig. 1 (*a*) Reaction of $[Pt(S_2CNPr^i_2)_2]$ and Ag^+; 0.070 cm^3 each of a 2.21×10^{-2} mol dm^{-3} solution of AgBF$_4$ in toluene was added successively to 100 cm^3 of a 1.13×10^{-5} mol dm^{-3} solution of $[Pt(S_2CNPr^i_2)_2]$ in CH$_2$Cl$_2$. The reaction was monitored in a 1 cm path length cell. (*b*) Plots of absorbance of the solution *versus* the Ag : Pt mole ratio of the reaction mixture

Fig. 2 (*a*) Reaction of $[Pt(S_2CNPr^i_2)_2]$ and $[Cu(MeCN)_4]^+$; 0.020 cm^3 each of a 2.25×10^{-2} mol dm^{-3} solution of $[Cu(MeCN)_4]BF_4$ was added successively to 100 cm^3 of a 2.25×10^{-5} mol dm^{-3} solution of $[Pt(S_2CNPr^i_2)_2]$ in CH$_2$Cl$_2$. The reaction was monitored in a 1 cm path length cell. (*b*) Plots of absorbance of the solution *versus* the Cu : Pt mole ratio of the mixture
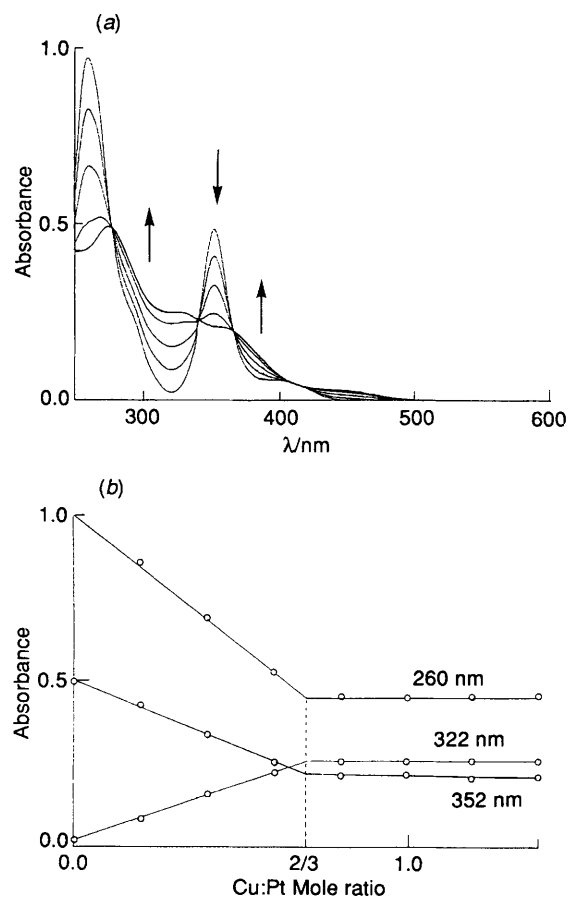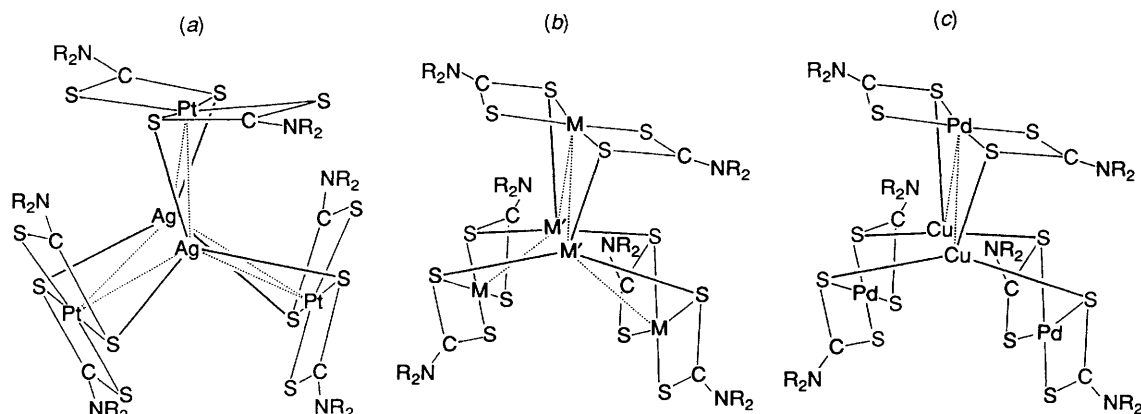

Fig. 3 Structures of discrete $[M_3(S_2CNR_2)_6M'_2]^{2+}$ ions. (*a*) Type II compounds $[Pt_3(S_2CNR_2)_6Ag_2]^{2+}$; (*b*) type III compounds $[M_3(S_2CNR_2)_6M'_2]^{2+}$ (M, M' = Pt, Cu and Pd, Ag); (*c*) type III compound $[Pd_3(S_2CNPr^n_2)_6Cu_2]^{2+}$

(a)

(b)

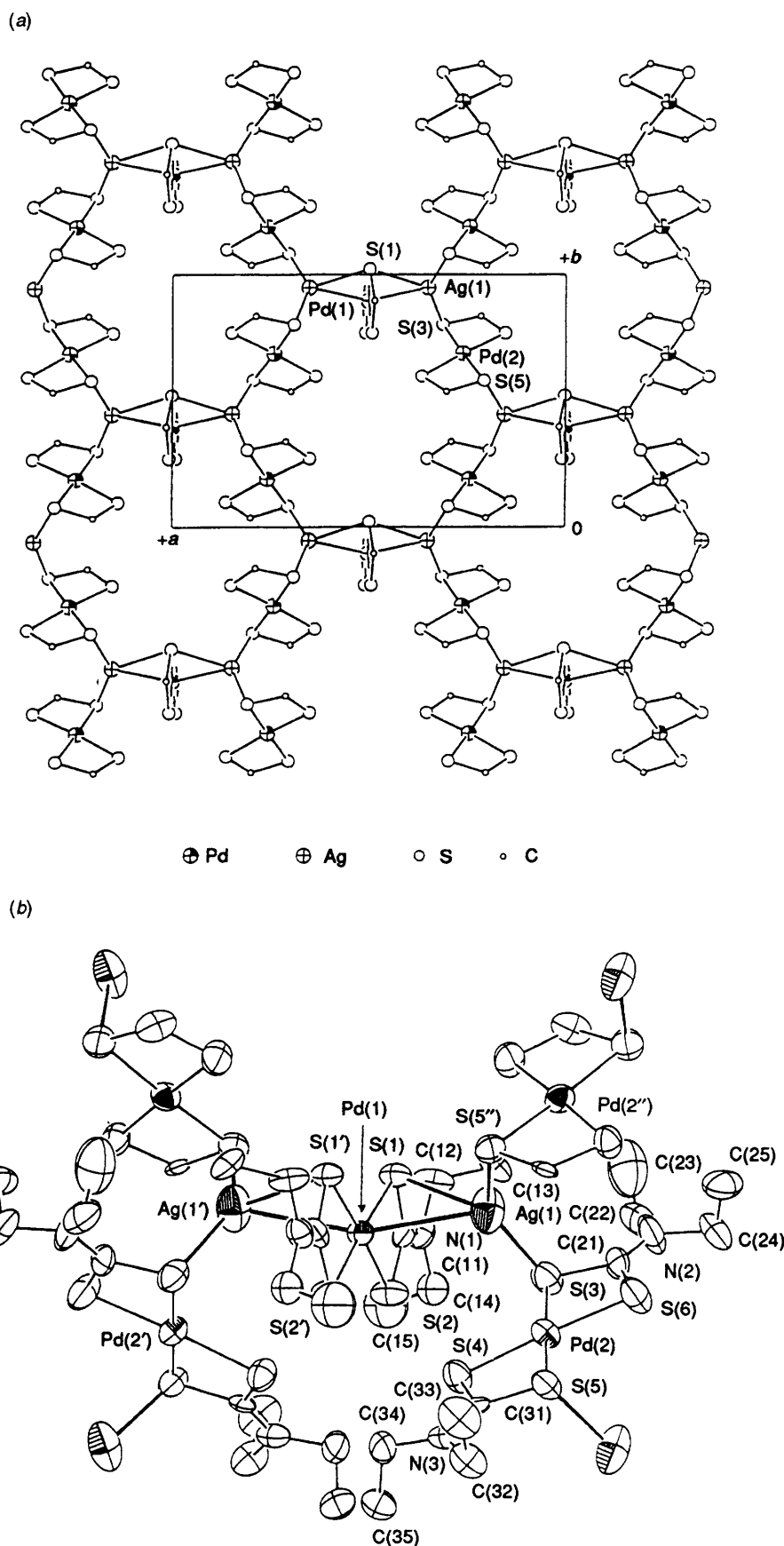**Fig. 4** Structure of $[\{Pd_3(S_2CNEt_2)_6Ag_2\}_n]^{2n+}$ in **1**. (a) Polymeric structure with alkyl carbon and nitrogen atoms omitted for clarity. The key atoms in an asymmetric unit are labelled. The view is along the c axis. (b) Part of the polymeric structure with some of the alkyl carbon and nitrogen atoms omitted for clarity. The thermal ellipsoids show 50% probability

Table 5 Positional parameters for $[Pt_3(S_2CNPr^i_2)_6Cu_2][BF_4]_2 \cdot 2CH_2Cl_2$ **4**

Atom	x	y	z	Atom	x	y	z
Pt(1)	−0.358 22(3)	−0.715 11(2)	−0.903 05(2)	C(31)	−0.161 4(8)	−0.864 4(4)	−0.759 5(5)
Pt(2)	−0.251 34(3)	−0.740 86(2)	−0.681 57(2)	C(32)	0.054 6(8)	−0.713 9(4)	−0.866 6(6)
Pt(3)	−0.069 87(3)	−0.782 32(2)	−0.809 49(2)	C(111)	−0.358 3(9)	−0.852 4(4)	−1.064 0(6)
Cu(1)	−0.322 4(1)	−0.783 75(5)	−0.803 20(7)	C(112)	−0.275(1)	−0.886 4(5)	−1.044 9(7)
Cu(2)	−0.172 8(1)	−0.697 77(5)	−0.835 03(7)	C(113)	−0.426(1)	−0.866 1(5)	−1.128 3(6)
Cl(1)	0.038 4(3)	−0.916 8(1)	−0.860 3(2)	C(114)	−0.505(1)	−0.872 0(5)	−0.979 5(8)
Cl(2)	0.201 5(3)	−0.851 0(2)	−0.881 9(2)	C(115)	−0.481(1)	−0.923 1(5)	−0.980 4(9)
Cl(3)	−0.122 4(3)	−0.501 4(2)	−0.490 9(2)	C(116)	−0.605(1)	−0.854 3(5)	−1.018 2(7)
Cl(4)	−0.287 5(3)	−0.481 4(2)	−0.592 5(2)	C(121)	−0.301(1)	−0.534 4(4)	−0.884 4(6)
S(11)	−0.456 7(2)	−0.782 4(1)	−0.897 5(1)	C(122)	−0.186(1)	−0.541 1(4)	−0.868 4(7)
S(12)	−0.295 2(2)	−0.766 2(1)	−0.981 8(1)	C(123)	−0.333(1)	−0.532 3(4)	−0.963 2(6)
S(13)	−0.272 3(2)	−0.645 2(1)	−0.918 6(2)	C(124)	−0.438(1)	−0.556 9(4)	−0.802 0(6)
S(14)	−0.429 9(2)	−0.661 3(1)	−0.830 8(2)	C(125)	−0.382(1)	−0.528 3(5)	−0.743 5(7)
S(21)	−0.420 0(2)	−0.753 9(1)	−0.719 2(1)	C(126)	−0.522(1)	−0.528 0(5)	−0.843 2(8)
S(22)	−0.296 4(2)	−0.809 0(1)	−0.626 1(1)	C(211)	−0.608 4(8)	−0.810 6(5)	−0.664 3(6)
S(23)	−0.093 7(2)	−0.724 0(1)	−0.629 9(1)	C(212)	−0.617(1)	−0.823 8(5)	−0.743 2(6)
S(24)	−0.206 4(2)	−0.670 1(1)	−0.730 0(1)	C(213)	−0.644(1)	−0.760 3(5)	−0.649 3(7)
S(31)	−0.203 0(2)	−0.834 0(1)	−0.835 1(1)	C(214)	−0.490(1)	−0.852 6(5)	−0.574 4(6)
S(32)	−0.062 8(2)	−0.834 2(1)	−0.717 9(2)	C(215)	−0.559(1)	−0.837 3(5)	−0.517 8(6)
S(33)	0.073 3(2)	−0.737 2(1)	−0.785 6(2)	C(216)	−0.510(1)	−0.902 5(5)	−0.600 9(7)
S(34)	−0.062 4(2)	−0.733 1(1)	−0.905 1(1)	C(221)	0.060 0(9)	−0.636 0(4)	−0.613 2(6)
F(1)	−0.287 2(7)	−0.454 6(3)	−0.259 6(4)	C(222)	0.019(1)	−0.634 4(5)	−0.539 8(6)
F(2)	−0.406 9(6)	−0.454 6(3)	−0.350 9(5)	C(223)	0.136 9(9)	−0.675 5(5)	−0.624 8(6)
F(3)	−0.350 4(7)	−0.386 0(3)	−0.301 2(4)	C(224)	−0.043 4(9)	−0.595 3(4)	−0.714 5(6)
F(4)	−0.249 6(7)	−0.429 5(3)	−0.363 8(4)	C(225)	0.040(1)	−0.596 5(4)	−0.764 4(6)
F(5)	−0.245 2(6)	−0.429 3(3)	−0.824 8(4)	C(226)	−0.045(1)	−0.549 0(4)	−0.673 5(7)
F(6)	−0.186 1(6)	−0.360 3(3)	−0.861 2(5)	C(311)	−0.142(1)	−0.929 5(4)	−0.676 8(6)
F(7)	−0.243 3(6)	−0.414 7(4)	−0.938 5(4)	C(312)	−0.221(1)	−0.939 5(5)	−0.623 9(6)
F(8)	−0.097 0(5)	−0.426 4(3)	−0.875 1(4)	C(313)	−0.089(1)	−0.974 6(4)	−0.698 0(7)
N(11)	−0.417 4(7)	−0.841 5(4)	−1.001 5(5)	C(314)	−0.276 9(9)	−0.933 8(4)	−0.779 0(6)
N(12)	−0.361 5(7)	−0.573 3(3)	−0.852 3(5)	C(315)	−0.243(1)	−0.948 6(5)	−0.849 7(6)
N(21)	−0.500 5(7)	−0.818 2(3)	−0.633 7(5)	C(316)	−0.378(1)	−0.907 1(4)	−0.783 2(7)
N(22)	−0.031 5(7)	−0.636 6(3)	−0.667 4(5)	C(321)	0.106(1)	−0.671 6(5)	−0.972 6(6)
N(31)	−0.194 5(7)	−0.906 2(3)	−0.739 9(5)	C(322)	0.017(1)	−0.639 4(5)	−0.985 7(8)
N(32)	0.120 4(7)	−0.687 1(3)	−0.897 2(5)	C(323)	0.108(1)	−0.715 5(5)	−1.020 5(6)
C(01)	0.139(1)	−0.882 9(6)	−0.819 0(7)	C(324)	0.220(1)	−0.675 7(5)	−0.856 3(6)
C(02)	−0.229(1)	−0.464 0(6)	−0.510 5(8)	C(325)	0.252(1)	−0.623 6(5)	−0.869 5(6)
C(11)	−0.391 6(8)	−0.803 4(4)	−0.966 9(6)	C(326)	0.301(1)	−0.712 1(5)	−0.872 2(8)
C(12)	−0.355 5(8)	−0.618 7(4)	−0.864 4(6)	B(1)	−0.324(1)	−0.431 3(5)	−0.318 8(8)
C(21)	−0.419 7(8)	−0.798 1(4)	−0.657 5(5)	B(2)	−0.192(1)	−0.407 5(6)	−0.875(1)
C(22)	−0.095 2(8)	−0.671 9(4)	−0.673 0(6)				
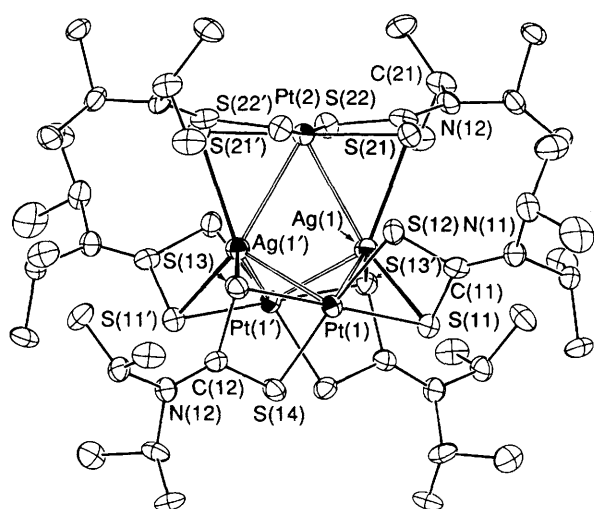
Fig. 5 ORTEP view of $[Pt_3(S_2CNPr^i_2)_6Ag_2]^{2+}$ in **7** with 50% probability

M $\cdots$ M′ interacting pairs with separations shorter than van der Waals contacts. Compounds of type III have two types

of co-ordination of $M(S_2CNR_2)_2$ to the two M′ atoms, and $[Pd_3(S_2CNPr^n_2)_6Ag_2]^{2+}$, $[Pt_3(S_2CNEt_2)_6Cu_2]^{2+}$, $[Pt_3(S_2CNPr^i_2)_6Cu_2]^{2+}$, $[Pt_3\{S_2CN(C_6H_{11})_2\}_6Cu_2]^{2+}$ and $[Pd_3(S_2CNPr^n_2)_6Cu_2]^{2+}$ belong to this category.

Type I complexes. The structure of complex **1** includes the two-dimensional cationic polymer$[\{Pd_3(S_2CNEt_2)_6Ag_2\}_n]^{2n+}$, which is shown in Fig. 4. The structure resembles that of the corresponding platinum derivative, $[\{Pt_3(S_2CNEt_2)_6$-$Ag_2\}_n]^{2n+}$, in compound **8**.[15] Both of the crystalline compounds consist of layers of two-dimensional cationic polymer and perchlorate anions. In the cationic polymer six $Pd(S_2CNEt_2)_2$ units and six Ag^+ ions form a large ring. Each of the Ag^+ ions is shared by three rings. Each of the $Pt(S_2CNEt_2)_2$ units bridges two Ag^+ ions by using the S atoms of the dithiocarbamato ligands. Table 9 summarizes the important distances in compound **1** together with those for **8** for comparison. The atom Pd(1), which is located on a crystallographic two-fold axis, bonds to two Ag atoms by using the *cis*-S atoms [S(1) and S(1′)]. The *trans*-S atoms around Pd(2) [S(3) and S(5)] connect two Ag atoms. The Ag atom bonds with three S atoms and the resulting AgS_3 is almost planar (the sum of the three S–Ag–S angles is 358.2°).

The bond distances and angles within each of the dithiocarbamate units in **1** and **8** are almost identical. The Pd(1)–Ag(1) distance is shorter than the van der Waals contact (3.30 Å). The other Pd–Ag separations are similar to the van der
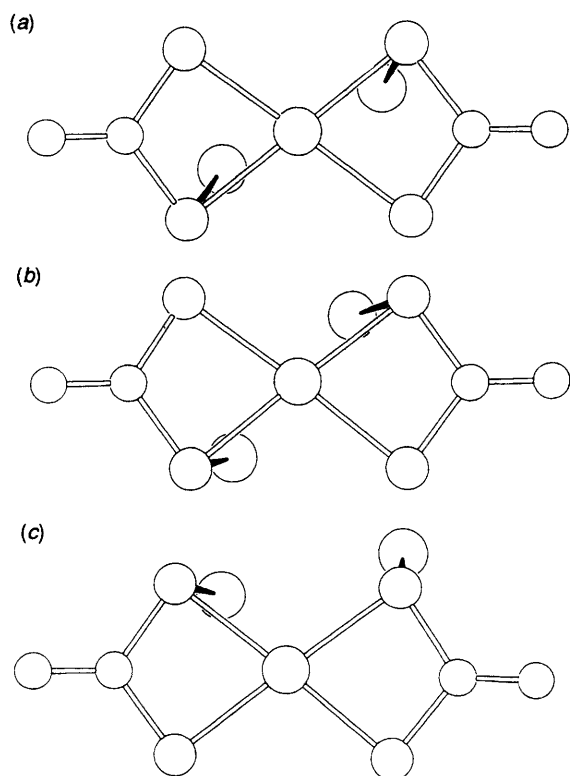
Fig. 6 (*a*) *trans* Mode co-ordination of $M(S_2CNR_2)_2$ in type II compounds and (*b*) *trans* and (*c*) *cis* mode co-ordinations of $M(S_2CNR_2)_2$ in type III compounds
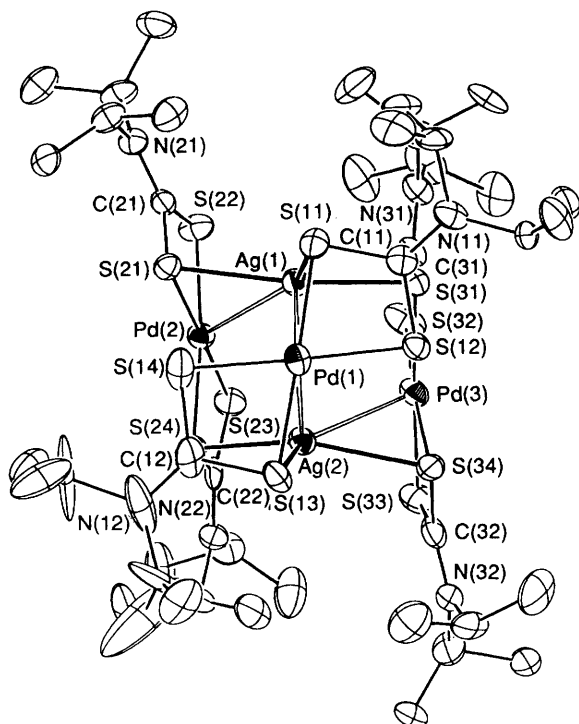

Fig. 8 ORTEP view of $[Pt_3(S_2CNPr^i_2)_6Cu_2]^{2+}$ in **4** with 50% probability

Fig. 9 ORTEP view (50% probability) of $[Pd_3(S_2CNPr^n_2)_6Cu_2]^{2+}$ in **6** with disordered alkyl carbon atoms omitted for clarity

Fig. 7 ORTEP view of $[Pd_3(S_2CNPr^i_2)_6Ag_2]^{2+}$ in **2** with 50% probability

Waals contact. On the other hand, $[\{Pt_3(S_2CNEt_2)_6Ag_2\}_n]^{2n+}$ has two short Pt–Ag distances [Pt(1)–Ag(1) 2.933(2) and Pt(2)–Ag(1) 3.046(2) Å] which are much shorter than the van der Waals contact (3.45 Å). All the Ag–S distances in **1** are
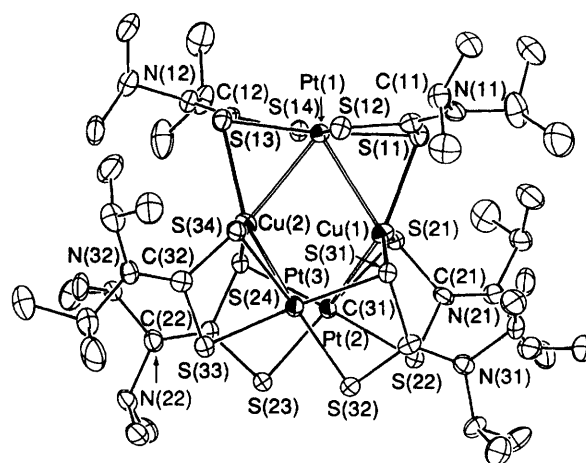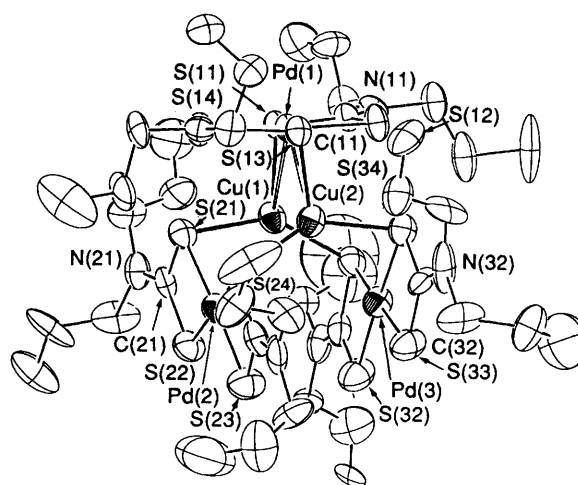
shorter than their corresponding distances in **8**. The Ag(1)–S(1) distance in **1** is shorter than the van der Waals contact, but the corresponding separation in **8** is longer than the contact. In summary the M–Ag separations are shorter in **8** whereas the S–Ag distances are shorter in **1**.

Type II complexes. Fig. 5 shows the structure and atomic numbering scheme of $[Pt_3(S_2CNPr^i_2)_6Ag_2]^{2+}$ in **7**, which belongs to type II. The atom Pt(2) is on the crystallographic two-fold axis. Table 10 lists selected distances and angles of this discrete cation. In the structure each $Pt(S_2CNPr^i_2)_2$ unit uses a pair of *trans*-S atoms to bond to the two silver atoms [Fig. 6(*a*)]. We define it as *trans* mode co-ordination. A pseudo-three-fold axis passes through the Ag atoms. This type of structure has been observed only for the Pt–Ag compounds **7** and $[Pt_3(S_2CNBu^n_2)_6Ag_2][ClO_4]_2$ **9** in which one of Ag atoms is weakly co-ordinated by a ClO_4^- ion.[16]

Type III complexes. The structure of $[Pd_3(S_2CNPr^i_2)_6-Ag_2]^{2+}$ (Fig. 7) in **2** is discrete, but differs from that of type II compounds as it does not have a pseudo-three-fold axis passing through the Ag $\cdots$ Ag axis. It is therefore classified as type III. Two Ag atoms are surrounded by three $Pd(S_2CNPr^i_2)_2$ units and each Ag atom is bonded by three S atoms. Two types of bonding mode exist for the $Pd(S_2CNPr^i_2)_2$ units [Fig. 6(*b*) and 6(*c*)]. The $Pd(S_2CNPr^i_2)_2$ unit with the palladium atom numbered Pd(1) uses a pair of *trans*-S atoms to bond to the silver atoms [Fig. 6(*b*)]. The co-ordination geometry around

Table 6   Positional parameters for [Pt$_3${S$_2$CN(C$_6$H$_{11}$)$_2$}$_6$Cu$_2$][PF$_6$]$_2$·2.73CH$_2$Cl$_2$ **5**

Atom	x	y	z	Atom	x	y	z
Pt(1)	0.071 98(3)	−0.871 10(7)	−0.221 91(3)	C(114)	−0.179 4(8)	−1.196(2)	−0.313 5(7)
Pt(2)	−0.091 99(3)	−0.538 38(7)	−0.280 47(3)	C(115)	−0.188(1)	−1.297(2)	−0.341 9(8)
Pt(3)	0.036 38(3)	−0.679 75(8)	−0.267 58(3)	C(116)	−0.175(1)	−1.279(2)	−0.381(1)
Cu(1)	−0.035 8(1)	−0.656 4(2)	−0.205 32(8)	C(117)	−0.201(1)	−1.177(2)	−0.408 7(8)
Cu(2)	−0.060 5(1)	−0.796 2(2)	−0.294 99(8)	C(118)	−0.189(1)	−1.069(2)	−0.377 9(9)
Cl(1)	−0.122 7(3)	−0.854 9(6)	−0.041 0(3)	C(119)	−0.259 0(7)	−0.967(2)	−0.315 1(6)
Cl(2)^a	−0.227 9(4)	−0.837(1)	−0.051 6(5)	C(120)	−0.279 8(8)	−1.065(2)	−0.298 0(7)
Cl(3)^b	−0.225(2)	−0.874(3)	−0.118(1)	C(121)	−0.336 0(8)	−1.037(2)	−0.297 0(7)
Cl(4)	−0.271 2(4)	−0.412(1)	−0.289 9(3)	C(122)	−0.371 9(9)	−1.001(2)	−0.341 2(7)
Cl(5)	−0.261 0(5)	−0.626(1)	−0.318 5(7)	C(123)	−0.353(1)	−0.900(2)	−0.359 2(7)
Cl(6)^a	−0.263 7(5)	−0.817(1)	−0.204 7(5)	C(124)	−0.296 6(8)	−0.932(2)	−0.360 8(7)
Cl(7)^a	−0.330 0(6)	−0.670(2)	−0.223 4(8)	C(201)	−0.137 2(7)	−0.435(2)	−0.148 7(6)
S(11)	−0.046 2(2)	−0.789 5(4)	−0.154 2(2)	C(202)	−0.097 1(7)	−0.518(2)	−0.117 9(6)
S(12)	0.015 4(2)	−0.918 5(5)	−0.186 1(2)	C(203)	−0.120 5(8)	−0.556(2)	−0.083 4(7)
S(13)	−0.099 2(2)	−0.974 4(5)	−0.284 8(2)	C(204)	−0.175 9(8)	−0.607(2)	−0.108 0(7)
S(14)	−0.162 0(2)	−0.841 1(5)	−0.255 5(2)	C(205)	−0.214 0(8)	−0.523(2)	−0.138 6(6)
S(21)	−0.116 7(2)	−0.573 2(4)	−0.222 3(2)	C(206)	−0.193 0(7)	−0.483(2)	−0.172 9(6)
S(22)	−0.069 0(2)	−0.382 9(5)	−0.237 7(2)	C(207)	−0.109 2(8)	−0.262(2)	−0.175 3(6)
S(23)	−0.072 4(2)	−0.493 0(5)	−0.339 5(2)	C(208)	−0.067 9(8)	−0.232(2)	−0.129 6(6)
S(24)	−0.125 7(2)	−0.680 5(5)	−0.329 5(2)	C(209)	−0.059 8(8)	−0.107(2)	−0.128 3(7)
S(31)	0.049 9(2)	−0.646 3(5)	−0.194 6(2)	C(210)	−0.114 7(8)	−0.046(2)	−0.137 0(7)
S(32)	0.057 3(2)	−0.498 8(5)	−0.256 7(2)	C(211)	−0.154 0(8)	−0.084(2)	−0.182 7(7)
S(33)	0.035 6(2)	−0.700 6(5)	−0.336 2(2)	C(212)	−0.163 0(8)	−0.213(2)	−0.185 7(6)
S(34)	0.021 0(2)	−0.866 9(5)	−0.284 0(2)	C(213)	−0.100 8(9)	−0.563(2)	−0.436 8(7)
P(1)	−0.201 1(2)	−0.215 7(6)	−0.060 1(2)	C(214)	−0.048(1)	−0.579(2)	−0.433 4(8)
P(2)	−0.369 0(6)	−0.264(1)	−0.431 6(3)	C(215)	−0.033 9(8)	−0.517(2)	−0.466 5(7)
F(1)	−0.179 4(5)	−0.296(1)	−0.019 3(4)	C(216)	−0.065(1)	−0.411(3)	−0.484(1)
F(2)	−0.155 7(5)	−0.132(1)	−0.033 1(4)	C(217)	−0.119(1)	−0.403(2)	−0.487 9(8)
F(3)	−0.240 0(6)	−0.163(2)	−0.042 1(5)	C(218)	−0.135 6(9)	−0.466(2)	−0.457 0(7)
F(4)	−0.246 5(6)	−0.298(1)	−0.086 6(5)	C(219)	−0.152(1)	−0.738(2)	−0.426 7(8)
F(5)	−0.162 0(5)	−0.270(1)	−0.079 2(4)	C(220)	−0.121(1)	−0.821(3)	−0.432(1)
F(6)	−0.219 2(5)	−0.136(1)	−0.100 7(4)	C(221)	−0.157(2)	−0.926(3)	−0.454(1)
F(7)	−0.406(1)	−0.345(2)	−0.417 0(8)	C(222)	−0.209(2)	−0.891(3)	−0.484(1)
F(8)	−0.334 4(7)	−0.234(1)	−0.383 5(4)	C(223)	−0.240(1)	−0.822(3)	−0.469(1)
F(9)	−0.408 9(8)	−0.177(2)	−0.433 7(6)	C(224)	−0.210(1)	−0.699(3)	−0.455(1)
F(10)	−0.402(1)	−0.292(2)	−0.480 8(5)	C(301)	0.095 6(7)	−0.465(2)	−0.126 2(6)
F(11)	−0.331(1)	−0.360(2)	−0.428 8(8)	C(302)	0.154 0(7)	−0.481(2)	−0.097 1(6)
F(12)	−0.337 4(6)	−0.183(2)	−0.448 4(6)	C(303)	0.157 9(8)	−0.502(2)	−0.048 6(7)
N(11)	0.052 1(6)	−0.863(1)	−0.101 2(5)	C(304)	0.135(1)	−0.409(2)	−0.033 5(8)
N(12)	−0.205 2(6)	−0.999(1)	−0.315 2(5)	C(305)	0.075(1)	−0.393(2)	−0.062 7(8)
N(21)	−0.115 2(6)	−0.387(1)	−0.179 6(5)	C(306)	0.070 0(9)	−0.366(2)	−0.110 4(8)
N(22)	−0.119 3(6)	−0.630(1)	−0.406 6(5)	C(307)	0.116 8(8)	−0.336(2)	−0.176 7(7)
N(31)	0.090 3(5)	−0.441(1)	−0.172 0(5)	C(308)	0.163 9(8)	−0.365(2)	−0.190 3(7)
N(32)	0.034 7(6)	−0.907(1)	−0.360 6(5)	C(309)	0.190(1)	−0.249(2)	−0.191 7(8)
C(11)	0.013 9(7)	−0.856(2)	−0.141 0(6)	C(310)	0.155(1)	−0.162(2)	−0.216 1(8)
C(12)	−0.162 4(7)	−0.946(2)	−0.289 9(6)	C(311)	0.108 2(9)	−0.145(2)	−0.203 2(7)
C(21)	−0.100 7(7)	−0.437(2)	−0.207 5(6)	C(312)	0.076(1)	−0.255(2)	−0.205 3(8)
C(22)	−0.107 2(7)	−0.604(2)	−0.364 9(6)	C(313)	0.046 6(9)	−0.865(2)	−0.400 0(7)
C(31)	0.068 5(7)	−0.512(2)	−0.203 9(6)	C(314)	0.105 4(9)	−0.892(2)	−0.388 7(7)
C(32)	0.026 8(7)	−0.838(2)	−0.332 3(6)	C(315)	0.118(1)	−0.850(2)	−0.429 4(8)
C(101)	0.051 1(7)	−0.817(2)	−0.059 2(6)	C(316)	0.077(1)	−0.882(2)	−0.473 0(8)
C(102)	0.010 8(7)	−0.884(2)	−0.047 0(6)	C(317)	0.023 4(9)	−0.854(2)	−0.478 2(7)
C(103)	0.017 3(7)	−0.844(2)	−0.000 5(6)	C(318)	0.005(1)	−0.904(2)	−0.442 5(8)
C(104)	0.009 1(8)	−0.722(2)	0.001 2(7)	C(319)	0.027(1)	−1.027(2)	−0.359 9(8)
C(105)	0.045 1(7)	−0.655(2)	−0.016 4(6)	C(320)	−0.033(1)	−1.055(2)	−0.375 6(8)
C(106)	0.038 2(7)	−0.695(2)	−0.062 5(6)	C(321)	−0.035(1)	−1.179(3)	−0.379(1)
C(107)	0.102 7(8)	−0.923(2)	−0.097 8(7)	C(322)	0.000(1)	−1.240(3)	−0.342(1)
C(108)	0.112 0(9)	−1.021(2)	−0.065 2(7)	C(323)	0.059(1)	−1.214(2)	−0.329 9(8)
C(109)	0.161(1)	−1.081(2)	−0.062 9(8)	C(324)	0.066(1)	−1.083(2)	−0.323 9(9)
C(110)	0.207(1)	−1.001(2)	−0.051 1(8)	C(401)	−0.185(1)	−0.894(3)	−0.070(1)
C(111)	0.198(1)	−0.908(2)	−0.081 5(8)	C(402)	−0.254(2)	−0.501(3)	−0.329(2)
C(112)	0.146 8(9)	−0.839(2)	−0.084 1(7)	C(403)^a	−0.309(1)	−0.812(3)	−0.183(1)
C(113)	−0.205 4(8)	−1.097(2)	−0.341 3(7)				

^{a} 73% occupancy. ^{b} 27% occupancy.

this unit is similar to that of the *trans* mode co-ordination in the type II compounds [Fig. 6(*a*)]. Important distances and angles are listed in Table 11 together with those for **6**, which is discussed later. A pseudo-two-fold axis exists through the Pd(1) atom perpendicular to its PdS$_4$ plane. The two Pd(1)–Ag

distances from the Pd(S$_2$CNPr$^i_2$)$_2$ unit co-ordinating in the *trans* mode are almost the same [2.928(1) and 3.001(1) Å] and shorter than the van der Waals contact. The Pd(S$_2$CNPr$^i_2$)$_2$ units around Pd(2) and Pd(3) use *cis*-S atoms [Fig. 6(*c*)]. This mode of co-ordination is designated the *cis* mode. Each of the
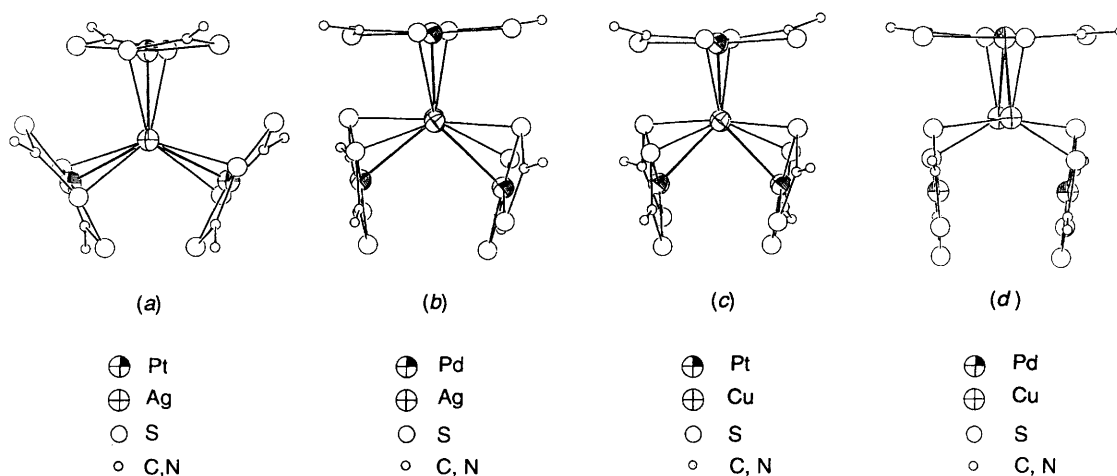
Fig. 10 Views through the M'···M' axis of (a) $[Pt_3(S_2CNPr^i_2)_6Ag_2]^{2+}$, (b) $[Pd_3(S_2CNPr^i_2)_6Ag_2]^{2+}$, (c) $[Pt_3(S_2CNPr^i_2)_6Cu_2]^{2+}$ and (d) $[Pd_3(S_2CNPr^n_2)_6Cu_2]^{2+}$. The alkyl groups are omitted for clarity

Table 7 Positional parameters for $[Pd_3(S_2CNPr^n_2)_6Cu_2][PF_6]_2 \cdot 0.5CH_2Cl_2 \cdot 0.5C_6H_{14}$ **6**

Atom	x	y	z	Atom	x	y	z
Pd(1)	0.401 6(1)	0.121 48(6)	0.008 2(2)	C(22)	0.158(1)	0.044(1)	0.125(2)
Pd(2)	0.186 3(1)	0.134 65(7)	0.143 9(2)	C(31)	0.157(1)	0.187(1)	−0.157(2)
Pd(3)	0.197 9(1)	0.096 75(7)	−0.169 4(2)	C(32)	0.231(1)	0.005(1)	−0.192(2)
Cu(1)	0.289 6(2)	0.177 4(1)	−0.004 0(3)	C(111)	0.419(1)	0.262 3(8)	−0.215(2)
Cu(2)	0.295 7(2)	0.058 5(1)	0.002 9(3)	C(112)	0.487(1)	0.276(1)	−0.195(3)
S(11)	0.399 4(3)	0.197 1(2)	−0.023 1(6)	C(113)	0.487(2)	0.327(1)	−0.169(3)
S(12)	0.408 1(4)	0.127 8(2)	−0.183 9(6)	C(114)	0.427(2)	0.200 8(9)	−0.358(2)
S(13)	0.404 4(4)	0.046 2(2)	0.042 2(6)	C(115)	0.362(2)	0.194(1)	−0.418(2)
S(14)	0.400 4(4)	0.115 8(2)	0.199 9(6)	C(116)	0.373(2)	0.182(1)	−0.544(2)
S(21)	0.269 7(4)	0.185 3(2)	0.179 8(6)	C(121)	0.413(1)	−0.018 7(8)	0.236(2)
S(22)	0.134 9(4)	0.202 7(2)	0.149 2(7)	C(122)	0.482(1)	−0.033 3(9)	0.205(2)
S(23)	0.100 5(4)	0.086 6(3)	0.113 2(8)	C(123)	0.530(1)	−0.023 1(9)	0.294(3)
S(24)	0.232 6(4)	0.063 9(2)	0.153 6(6)	C(124)	0.405(1)	0.044(1)	0.383(2)
S(31)	0.238 9(4)	0.168 9(2)	−0.167 4(6)	C(125)	0.331(2)	0.044(1)	0.413(2)
S(32)	0.107 1(4)	0.141 8(3)	−0.161 2(8)	C(126)	0.319(2)	0.047(1)	0.525(4)
S(33)	0.152 8(4)	0.026 8(3)	−0.181 8(8)	C(211)	0.162(1)	0.297 9(8)	0.233(3)
S(34)	0.286 7(4)	0.048 8(2)	−0.183 4(6)	C(212)	0.149(2)	0.300(1)	0.367(3)
P(1)	0.590 4(5)	0.115 5(3)	0.491 4(8)	C(213)	0.093(2)	0.330(1)	0.374(3)
P(2)	0.390 3(8)	0.341 1(4)	0.495(1)	C(214)	0.287(2)	0.285(1)	0.223(3)
F(11)	0.576(1)	0.165 0(5)	0.510(1)	C(215)	0.307(2)	0.307(1)	0.100(3)
F(12)	0.663(1)	0.129 0(8)	0.487(2)	C(216)	0.371(2)	0.328(1)	0.099(3)
F(13)	0.601(1)	0.108 3(6)	0.615(2)	C(221)	0.192(2)	−0.034(1)	0.122(3)
F(14)	0.606(1)	0.067 3(6)	0.476(2)	C(222)	0.204(2)	−0.045(1)	0.238(3)
F(15)	0.517(1)	0.105 4(8)	0.503(2)	C(223)	0.259(2)	−0.082(1)	0.236(4)
F(16)	0.587(2)	0.122 2(8)	0.371(2)	C(224)	0.074(2)	−0.014(1)	0.088(2)
F(21)	0.410(1)	0.387 2(7)	0.530(2)	C(225)	0.038(2)	−0.039(1)	0.177(3)
F(22)	0.410(2)	0.348(1)	0.387(2)	C(226)	0.023(2)	−0.009(2)	0.269(5)
F(23)	0.323(1)	0.364 5(8)	0.464(2)	C(311)	0.184(1)	0.262(1)	−0.136(2)
F(24)	0.360(2)	0.298 2(8)	0.465(3)	C(312)	0.215 1	0.279 2	−0.244 5
F(25)	0.360(1)	0.336 4(8)	0.612(2)	C(313)	0.236 1	0.313 2	−0.249 2
F(26)	0.449(1)	0.317 9(8)	0.537(2)	C(314)	0.068(1)	0.237(1)	−0.130(3)
N(11)	0.418(1)	0.213 1(7)	−0.240(2)	C(315)	0.038(2)	0.257(2)	−0.240(4)
N(12)	0.408(1)	0.031 0(7)	0.262(2)	C(316)[a]	−0.022(4)	0.265(3)	−0.243(7)
N(21)	0.219(1)	0.268 0(7)	0.211(2)	C(317)[b]	0.038(3)	0.232(2)	−0.325(6)
N(22)	0.142(1)	0.000(1)	0.114(2)	C(321)	0.319(1)	−0.051(1)	−0.199(3)
N(31)	0.136(1)	0.227 9(8)	−0.146(2)	C(322)	0.337(2)	−0.068(1)	−0.085(3)
N(32)	0.251(2)	−0.038 2(8)	−0.206(2)	C(323)	0.407(2)	−0.079(1)	−0.091(3)
C(11)	0.410(1)	0.183 4(8)	−0.163(2)	C(324)	0.193(1)	−0.070 7(9)	−0.219(3)
C(12)	0.405(1)	0.059 9(8)	0.177(2)	C(325)	0.182(2)	−0.081(1)	−0.354(4)
C(21)	0.209(1)	0.225 1(8)	0.183(2)	C(326)	0.165(3)	−0.058(2)	−0.442(4)

[a] 33% occupancy. [b] 67% occupancy.

Pd($S_2CNPr^i_2$)$_2$ units co-ordinating in the *cis* mode has one short and one long Pd–Ag distance. The Pd(2) atom seems to be attracted toward Ag(1) and Pd(3) toward Ag(2). The separations of Pd(2) from Ag(2) and Pd(3) from Ag(1) are

longer than the van der Waals contact, and no direct bonding interaction is likely between them.

We examined the structures of three Pt–Cu complexes. Fig. 8 shows the structure and the numbering scheme of

Table 8 Positional parameters for $[Pt_3(S_2CNPr^i_2)_6Ag_2][BF_4]_2$ **7**

Atom	x	y	z
Pt(1)	0.564 73(4)	0.224 62(1)	0.248 73(2)
Pt(2)	$\frac{3}{4}$	$\frac{1}{4}$	0.431 13(3)
Ag(1)	0.789 65(8)	0.202 54(3)	0.307 38(4)
S(11)	0.645 1(3)	0.154 0(1)	0.229 0(1)
S(12)	0.486 4(3)	0.178 8(1)	0.330 1(1)
S(13)	0.482 8(3)	0.294 7(1)	0.268 5(1)
S(14)	0.615 5(3)	0.267 4(1)	0.157 4(1)
S(21)	0.764 2(3)	0.172 0(1)	0.432 5(1)
S(22)	0.949 3(3)	0.235 3(1)	0.439 1(1)
F(1)	0.139 4(7)	0.027 9(2)	0.112 3(4)
F(2)	0.237 7(7)	0.069 9(2)	0.037 8(4)
F(3)	0.267 1(8)	−0.005 4(3)	0.042 5(4)
F(4)	0.334 0(8)	0.039 5(4)	0.123 8(5)
N(11)	0.535 5(8)	0.090 7(3)	0.308 2(4)
N(12)	0.497 7(8)	0.346 3(3)	0.156 6(4)
N(21)	0.985 5(8)	0.146 1(3)	0.465 1(4)
C(11)	0.553(1)	0.132 9(4)	0.292 1(5)
C(12)	0.527(1)	0.309 9(4)	0.188 2(5)
C(21)	0.915(1)	0.178 3(4)	0.448 0(5)
C(111)	0.609(1)	0.052 1(4)	0.282 5(5)
C(112)	0.739(1)	0.059 2(4)	0.298 5(6)
C(113)	0.584(1)	0.044 3(4)	0.208 5(6)
C(114)	0.443(1)	0.080 9(4)	0.360 0(6)
C(115)	0.506(1)	0.065 2(5)	0.423 8(6)
C(116)	0.361(1)	0.044 4(5)	0.331 4(7)
C(121)	0.553(1)	0.354 0(4)	0.089 0(5)
C(122)	0.605(1)	0.402 1(4)	0.084 4(6)
C(123)	0.464(1)	0.342 2(4)	0.036 6(5)
C(124)	0.408(1)	0.379 6(4)	0.179 4(6)
C(125)	0.457(1)	0.409 3(4)	0.235 3(6)
C(126)	0.288(1)	0.356 5(4)	0.196 1(6)
C(211)	1.112(1)	0.153 1(4)	0.484 7(6)
C(212)	1.186(1)	0.170 5(5)	0.425 6(6)
C(213)	1.121(1)	0.183 2(4)	0.545 9(6)
C(214)	0.939(1)	0.097 9(4)	0.467 8(5)
C(215)	0.930(1)	0.084 5(4)	0.542 4(5)
C(216)	1.017(1)	0.066 0(4)	0.426 7(6)
B(1)	0.246(2)	0.033 8(5)	0.079 5(8)

Table 9 Selected distances (Å) and angles (°) in $[M_3(S_2CNEt_2)_6Ag_2]$-$[ClO_4]_2$ (M = Pd **1** or Pt **8**)[a]

	M = Pd	M = Pt[b]
M(1)–Ag(1)	3.073(2)	2.933(2)
M(2)–Ag(1)	3.283(3)	3.046(2)
M(2″)–Ag(1)	3.287(3)	3.511(2)
Ag(1)–S(1)	2.826(6)	3.029(6)
Ag(1)–S(3)	2.496(7)	2.546(7)
Ag(1)–S(5″)	2.451(6)	2.480(6)
M(1)–S(1)	2.325(5)	2.317(4)
M(1)–S(2)	2.306(5)	2.316(4)
M(2)–S(3)	2.337(6)	2.321(4)
M(2)–S(4)	2.316(5)	2.320(3)
M(2)–S(5)	2.320(6)	2.327(4)
M(2)–S(6)	2.305(6)	2.302(4)
Ag(1)–M–Ag(1)	158.3(1)	166.8(1)
S(1)–Ag(1)–S(3)	110.1(2)	—
S(1)–Ag(1)–S(5″)	105.3(2)	—
S(3)–Ag(1)–S(5″)	142.8(2)	140.9(1)

[a] (″): $1 - x, y, \frac{3}{2} - z$. [b] From ref. 15.

Table 10 Selected bond distances (Å) and angles (°) for $[Pt_3(S_2CNPr^i_2)_6Ag_2]^{2+}$ in **7** *

Pt(1)–Ag(1)	2.895(1)	Pt(1)–S(11)	2.321(3)
Pt(1)–Ag(1′)	2.972(1)	Pt(1)–S(12)	2.316(3)
Pt(2)–Ag(1)	2.911(1)	Pt(1)–S(13)	2.316(3)
Ag(1)–Ag(1′)	2.960(2)	Pt(1)–S(14)	2.317(3)
Ag(1)–S(11)	2.702(3)	Pt(2)–S(21)	2.323(3)
Ag(1)–S(13′)	2.705(3)	Pt(2)–S(22)	2.313(3)
Ag(1)–S(21)	2.707(3)		

S(11)–Ag(1)–S(13′)	115.24(9)
S(11)–Ag(1)–S(21)	107.85(9)
S(13′)–Ag(1)–S(21)	112.63(9)

* ('): $\frac{3}{2} - x, \frac{1}{2} - y, z$.

Table 11 Selected bond distances (Å) and angles (°) for $[Pd_3(S_2CNPr^i_2)_6Ag_2]^{2+}$ in **2** and $[Pd_3(S_2CNPr^n_2)_6Cu_2]^{2+}$ in **6**

	$[Pd_3(S_2CNPr^i_2)_6Ag_2]^{2+}$	$[Pd_3(S_2CNPr^n_2)_6Cu_2]^{2+}$
Pd(1)–M(1)	2.928(1)	2.864(4)
Pd(1)–M(2)	3.001(1)	2.896(4)
Pd(2)–M(1)	2.934(1)	3.058(4)
Pd(3)–M(2)	2.911(1)	3.110(4)
Pd(2)–M(2)	3.466(1)	3.640(4)
Pd(3)–M(1)	3.587(1)	3.669(4)
M(1)–M(2)	3.093(1)	3.598(4)
M(1)–S(11)	2.764(3)	2.351(8)
M(1)–S(21)	2.530(3)	2.256(8)
M(1)–S(31)	2.477(3)	2.237(8)
M(2)–S(13)	2.662(3)	2.320(8)
M(2)–S(24)	2.468(3)	2.234(8)
M(2)–S(34)	2.563(3)	2.263(8)
Pd(1)–S(11)	2.306(3)	2.319(7)
Pd(1)–S(12)	2.335(3)	2.318(7)
Pd(1)–S(13)	2.332(3)	2.315(7)
Pd(1)–S(14)	2.314(3)	2.307(7)
Pd(2)–S(21)	2.343(3)	2.341(8)
Pd(2)–S(22)	2.323(3)	2.314(8)
Pd(2)–S(23)	2.307(3)	2.318(9)
Pd(2)–S(24)	2.324(3)	2.345(7)
Pd(3)–S(31)	2.333(3)	2.340(8)
Pd(3)–S(32)	2.301(3)	2.316(9)
Pd(3)–S(33)	2.318(3)	2.315(8)
Pd(3)–S(34)	2.327(3)	2.341(8)
S(11)–M(1)–S(21)	100.50(9)	104.1(3)
S(11)–M(1)–S(31)	99.97(9)	113.1(3)
S(21)–M(1)–S(31)	155.54(9)	141.7(3)
S(13)–M(2)–S(24)	107.03(9)	114.2(3)
S(13)–M(2)–S(34)	94.99(9)	105.0(3)
S(24)–M(2)–S(34)	148.67(9)	139.6(3)

are similar to that of **4**. Selected distances in **3**, **4** and **5** are listed in Table 12.

The structure of $[Pd_3(S_2CNPr^n_2)_6Cu_2]^{2+}$ in **6** is shown in Fig. 9. Important distances and angles are already listed in Table 11. This structure is classified as type III and is similar to those of $[Pd_3(S_2CNPr^i_2)_6Ag_2]^{2+}$ in **2** and $[Pt_3(S_2CNR_2)_6Cu_2]^{2+}$ (R = Et, Pr^i or C_6H_{11}) in **3**, **4** and **5** except that only two Pd–Cu distances in this compound are shorter than the van der Waals contact. The two short Pd–Cu distances extend from the $Pd(S_2CNPr^n_2)_2$ unit co-ordinating in the *trans* mode [Pd(1)].

M–M′ *Bond distances in discrete cations.* The type II compound **7** has six Pt–Ag distances [2.895(1)–2.972(1) Å] which are shorter than the van der Waals contact. On the other hand the type III compound **2** has four short Pd–Ag distances [2.911(1)–3.001(1) Å]. The M–Cu (M = Pt or Pd) compounds belong to type III. Four Pt–Cu [2.737(3) (in **5**)–2.921(3) Å (in **3**)] and two Pd–Cu distances [2.864(4) and 2.896(4) Å in **6**] in each are shorter than the van der Waals contacts (3.15 Å for

$[Pt_3(S_2CNPr^i_2)_6Cu_2]^{2+}$ in **4**. The structure is similar to that of $[Pd_3(S_2CNPr^i_2)_6Ag_2]^{2+}$ in **2** and the cation is classified as type III. The platinum dithiocarbamate unit of Pt(1) co-ordinates in the *trans* mode with the Cu atoms and the other two units in the *cis* mode. There are four short Pt–Cu distances [Pt(1)–Cu(1), Pt(1)–Cu(2), Pt(2)–Cu(1) and Pt(3)–Cu(2)] in this compound. The structures of the other Pt–Cu complexes examined (**3** and **5**)

Pt–Cu and 3.00 Å for Pd–Cu). These results show a trend that the bonding interaction between M and M' is greater for Pt and Ag than that for Pd and Cu.

Fig. 10 shows a comparison of the distortion in [M^{II}-(S_2CNR_2)$_2$] units. Table 13 summarizes the deviation of M from its S_4 best-plane. Each platinum dithiocarbamate unit in the Pt–Ag compound 7 is bent from planarity [Fig. 10(*a*)] and the Pt atoms are shifted toward the Ag atoms from the planes (0.095, 0.100 Å). In the Pd–Ag compound 2 the Pd atoms are also shifted toward the Ag atoms [Fig. 10(*b*)], but the shifts are smaller (0.044–0.088 Å) than those of the Pt atoms in 7. Each of the Pt–Cu compounds, 3, 4 and 5, includes three appreciably bent bis(dithiocarbamato)platinum moieties [*cf.* Fig. 10(*c*)]. The deviations of the Pt atoms from their S_4 planes (0.045–0.141 Å) are similar to those of the Pt–Ag compounds. On the other hand, the distortion is small in the Pd–Cu compound 6 [Fig. 10(*d*)]. These observations also support the existence of the bonding interaction between M and M', which is greater for Pt and Ag than for Pd and Cu.

XPS.—The binding energies of [$M_3(S_2CNR_2)_6M'_2$]$^{2+}$ are summarized in Table 14 together with those of free [$M(S_2CNR_2)_2$] for comparison. In the Pt–Ag compounds the Pt 4f$_{\frac{7}{2}}$ peaks are observed between 72.1 and 72.3 eV which are 0.5–0.6 eV larger than those of free [Pt(S_2CNR_2)$_2$]. The Pt 4f$_{\frac{7}{2}}$ binding energy of [$Pt_3(S_2CNEt_2)_6Ag_2$][ClO_4]$_2$, which belongs to type I, is no different from those of type II compounds with

discrete structure. The Pt 4f$_{\frac{7}{2}}$ binding energies of the Pt–Cu compounds (type III) are also 0.5–0.6 eV lower than those of free [Pt(S_2CNR_2)$_2$]. The palladium complexes [$Pd_3(S_2$-$CNR_2)_6M'_2$]X_2 (M' = Ag or Cu) also showed low-energy shifts of the Pd 3d$_{\frac{5}{2}}$ peaks (0.2–0.5 eV) and no significant difference was observed between those of the polymer and the discrete compounds. The difference in Ag 3d$_{\frac{5}{2}}$ binding energy between the Pt–Ag and the Pd–Ag compounds is within experimental error. The difference between the Cu 3p$_{\frac{3}{2}}$ binding energies of both of the Pt–Cu and Pd–Cu compounds was also negligible. The binding energy of S 2p$_{\frac{3}{2}}$ in [$M_3(S_2CNR_2)_6M'_2$]X_2 is 0.1–0.6 eV smaller than that of the corresponding free [$M(S_2CNR_2)_2$]. These data imply that electron density is delocalized to the M' atoms from the M and S atoms. However, it is difficult to estimate the extent of electron delocalization and the existence of direct M–M' bonding from the XPS data.

Platinum-195 NMR.—Platinum-195 NMR was measured for [$Pt_3(S_2CNBu^n_2)_6Ag_2$][BF_4]$_2$, [$Pt_3(S_2CNBu^n_2)_6Ag_2$][ClO_4]$_2$ 9, [$Pt_3(S_2CNBu^n_2)_6Cu_2$][BF_4]$_2$ and [$Pt_3(S_2CNBu^n_2)_6Cu_2$]-[PF_6]$_2$ in CH$_2$Cl$_2$. The mixed-metal compounds are sufficiently soluble in CH$_2$Cl$_2$ to record their ^{195}Pt NMR spectra. The compound [$Pt_3(S_2CNBu^n_2)_6Ag_2$][BF_4]$_2$ in CH$_2$Cl$_2$ showed a 1:2:1 triplet at δ −3348 *vs.* external H$_2$PtCl$_6$ in D$_2$O with a ^{195}Pt–^{107,109}Ag coupling constant of 194 Hz at room temperature. This is consistent with crystal structure of [Pt$_3$-($S_2CNPr^i_2)_6Ag_2$][BF_4]$_2$ in which each of the platinum atoms is bonded to two (almost) equivalent silver atoms ($I = \frac{1}{2}$). The signal of [$Pt_3(S_2CNBu^n_2)_6Ag_2$][ClO_4]$_2$ in CH$_2$Cl$_2$ was a broad singlet at room temperature and a broad 1:2:1 triplet [J(Pt–Ag) *ca.* 200 Hz] centred at δ −3361 at 223 K. In the crystal of 9 one ClO$_4$ moiety is weakly co-ordinated to a Ag atom.[16] These temperature-dependent spectra indicate an exchange equilibrium for the co-ordination of ClO$_4$ to Ag or an intermolecular exchange reaction of Ag$^+$ ions probably promoted by the co-ordination of ClO$_4$. A singlet peak was observed for [$Pt_3(S_2CNBu^n_2)_6Cu_2$][BF_4]$_2$ and [$Pt_3(S_2CN$-Bu$^n_2)_6Cu_2$][PF_6]$_2$ in CH$_2$Cl$_2$ at room temperature. When the temperature was lowered to 227 K, the peaks broadened, but did not split. These observations show that the structure containing geometrically inequivalent Pt atoms of these type III Pt–Cu compounds is not frozen in solution or that the solution structure of [$Pt_3(S_2CNBu^n_2)_6Cu_2$]$^{2+}$ differs from that in the crystal.

The ^{195}Pt chemical shifts of [Pt($S_2CNBu^n_2)_2$], [$Pt_3(S_2CN$-Bu$^n_2)_6Cu_2$]$^{2+}$ and [$Pt_3(S_2CNBu^n_2)_6Ag_2$]$^{2+}$ in CH$_2$Cl$_2$ are δ −3829, −3553 and −3348, respectively. A reasonable explanation for these observations is that the extent of electron delocalization from the Pt atom to the Ag atom is greater than that from the Pt to the Cu atoms.

Table 15 summarizes the ^{195}Pt–^{107,109}Ag coupling constants for various complexes which have been reported to have a Pt–Ag bond. They are in the range 165–811 Hz.[3,4,28–32] The values of *ca.* 200 Hz for the present [$Pt_3(S_2CNBu^n_2)_6Ag_2$]$^{2+}$ cations are similar to those in [{2,6-(Me$_2$NCH$_2$)$_2$C$_6$H$_3$}Pt-(*p*-MeC$_6$H$_4$NCHNR)AgBr] (R = Me, Et, Pr^i or *p*-tolyl)[32] and [{Pt(PPr$^i_3$)$_3$(CO)$_3$}$_2$Ag]$^+$.[30] This result supports the existence of a significant bonding interaction between the Pt and the Ag atoms in the present complexes.

Table 12 Selected bond distances (Å) and angles (°) for [$Pt_3(S_2CNR_2)_6Cu_2$]$^{2+}$ (R = Et 3, Pr^i 4 or C$_6$H$_{11}$ 5)

	R = Et	R = Pr^i	R = C$_6$H$_{11}$
Pt(1)–Cu(1)	2.859(3)	2.772(2)	2.806(3)
Pt(1)–Cu(2)	2.751(3)	2.749(2)	2.737(3)
Pt(2)–Cu(1)	2.854(3)	2.765(2)	2.794(3)
Pt(3)–Cu(2)	2.921(3)	2.796(2)	2.849(3)
Pt(2)–Cu(2)	3.426(3)	3.455(1)	3.377(4)
Pt(3)–Cu(1)	3.369(3)	3.358(2)	3.394(3)
Cu(1)–Cu(2)	3.169(4)	3.239(2)	3.289(4)
Cu(1)–S(11)	2.419(6)	2.461(3)	2.461(6)
Cu(1)–S(21)	2.298(6)	2.318(3)	2.313(6)
Cu(1)–S(31)	2.234(6)	2.254(3)	2.248(5)
Cu(2)–S(13)	2.569(6)	2.513(3)	2.520(6)
Cu(2)–S(24)	2.246(6)	2.263(3)	2.233(6)
Cu(2)–S(34)	2.270(6)	2.303(3)	2.298(6)
Pt(1)–S(11)	2.331(5)	2.328(3)	2.319(5)
Pt(1)–S(12)	2.323(6)	2.312(3)	2.311(5)
Pt(1)–S(13)	2.322(5)	2.326(3)	2.318(5)
Pt(1)–S(14)	2.322(6)	2.328(3)	2.322(5)
Pt(2)–S(21)	2.345(5)	2.331(3)	2.331(5)
Pt(2)–S(22)	2.321(5)	2.319(3)	2.326(6)
Pt(2)–S(23)	2.306(5)	2.303(3)	2.304(5)
Pt(2)–S(24)	2.336(5)	2.323(3)	2.332(5)
Pt(3)–S(31)	2.328(5)	2.323(3)	2.355(5)
Pt(3)–S(32)	2.316(5)	2.310(3)	2.297(6)
Pt(3)–S(33)	2.332(6)	2.312(3)	2.295(5)
Pt(3)–S(34)	2.348(5)	2.336(3)	2.370(6)
S(11)–Cu(1)–S(21)	99.7(2)	96.2(1)	96.2(2)
S(11)–Cu(1)–S(31)	104.9(2)	106.8(1)	108.7(2)
S(21)–Cu(1)–S(31)	148.0(2)	150.0(1)	149.9(2)
S(13)–Cu(2)–S(24)	106.3(2)	104.3(1)	109.2(2)
S(13)–Cu(2)–S(34)	102.5(2)	101.8(1)	94.9(2)
S(24)–Cu(2)–S(34)	143.7(2)	149.5(1)	149.9(2)

Table 13 Deviation (Å) of Group 10 metal atoms from the best planes of their surrounding sulfur atoms in discrete [$M_3(S_2CNR_2)_6M'_2$]$^{2+}$ ions

M–M'–R	Pt—Ag–Pr^i	Pd–Ag–Pr^i	Pt–Cu–Et	Pt–Cu–Pr^i	Pt–Cu–C$_6$H$_{11}$	Pd–Cu–Pr^n
	7	2	3	4	5	6
Type	II	III	III	III	III	III
M(1)	0.100	0.044	0.045	0.110	0.141	0.029
M(2)	0.095	0.088	0.083	0.118	0.125	0.068
M(3)		0.063	0.069	0.106	0.111	0.049

Table 14 XPS binding energies of $[M_3(S_2CNR_2)_6M'_2]X_2$

Complex						Binding energy/eV			
M	M'	R	X		Type	Pt $4f_{\frac{7}{2}}$	Ag $3d_{\frac{5}{2}}$	Cu $3p_{\frac{3}{2}}$	S $2p_{\frac{3}{2}}$
Pt	Ag	Et	ClO_4	8	I	72.1	368.1		162.3
Pt	Ag	Pr^i	BF_4	7	II	72.2	368.1		162.3
Pt	Ag	Pr^n	BF_4			72.3	368.1		162.4
Pt	Ag	Bu^n	ClO_4	9	II	72.3	368.1		162.4
Pt	Cu	Et	BF_4	4	III	72.1		932.8	162.6
Pt	Cu	Pr^i	BF_4	3	III	72.2		933.0	162.5
Pt	Cu	Pr^i	PF_6			72.2		933.1	162.4
Pt	Cu	C_6H_{11}	PF_6	5	III	72.0		932.8	162.4
Pt *		Et				71.6			162.0
Pt *		Pr^i				71.6			162.0
Pt *		Pr^n				71.6			162.0
Pt *		Bu^n				71.8			162.0
M	M'	R	X		Type	Pd $3d_{\frac{5}{2}}$	Ag $3d_{\frac{5}{2}}$	Cu $3p_{\frac{3}{2}}$	S $2p_{\frac{3}{2}}$
Pd	Ag	Et	ClO_4	1	I	337.1	367.9		162.1
Pd	Ag	Pr^i	BF_4	2	III	337.1	367.9		161.8
Pd	Ag	Pr^n	ClO_4			337.2	368.0		162.0
Pd	Ag	Bu^n	BF_4			337.1	368.0		162.0
Pd	Cu	Pr^n	BF_4			337.1		932.8	162.1
Pd	Cu	Pr^n	PF_6	6	III	337.1		932.7	162.2
Pd	Cu	Bu^n	BF_4			337.1		932.8	162.2
Pd	Cu	C_6H_{11}	BF_4			337.0		932.7	162.2
Pd *		Et				336.9			161.8
Pd *		Pr^i				336.6			161.7
Pd *		Pr^n				336.9			161.7
Pd *		Bu^n				336.8			161.8

* Free $[M(S_2CNR_2)_2]$ complex.

Table 15 $^{195}Pt-^{107,109}Ag$ coupling constants and Pt–Ag bond lengths of various complexes

Complex	J/Hz	$d(Pt-Ag)/Å$	Ref.
$[PtAg\{Au(PPh_3)\}_8]^{3+}$	717,^{a} 811^b	2.722(5)	28
$[Pt(CO)Ag\{Au(PPh_3)\}_8]^{3+}$	370	2.762(3)	28
$[Pt(CO)Ag_2\{Au(PPh_3)\}_7]^{3+}$	415	c	29
$[\{Pt(PPr^i_3)_3(CO)_3\}_2Ag]^+$	190	2.825(2)–2.853(2)	30
$[(Et_3P)_2(C_6Cl_5)Pt(H)Ag(OH_2)]^+$	739	2.750(3)	3
$[\{(Et_3P)_2(C_6Cl_5)Pt(H)\}_2Ag]^+$	554	2.791(1)	3
$[(R_3P)_2(C_6Cl_5)Pt(H)Ag(PR'_3)]^{+d}$	409–440	c	4
$[PtMe_2(bipy)Ag(PPh_3)]^{+e}$	680	c	31
$[(L)Pt(p-MeC_6H_4NCHNR)AgBr]^f$	165–173^b	c	32
$[Pt_3(S_2CNBu^n_2)_6Ag_2]^{2+}$	194	2.895(1)–2.972(1)^g	This work

^{a} $J(^{195}Pt-^{107}Ag)$. ^{b} $J(^{195}Pt-^{109}Ag)$. ^{c} No crystal structure. ^{d} R, R' = Et, Pr^i; Et, C_6H_{11}; Me, Pr^i. ^{e} bipy = 2,2'-bipyridine. ^{f} L = 2,6-$(Me_2NCH_2)_2C_6H_3^-$, R = Me, Et, Pr^i or C_6H_4Me-p. ^{g} Distances in $[Pt_3(S_2CNPr^i_2)_6Ag_2][BF_4]_2$.

Conclusion

The following trends have been observed in crystal structures of the $[M_3(S_2CNR_2)_6M'_2]^{2+}$ compounds: the number of M $\cdots$ M' pairs that have contacts shorter than the corresponding van der Waals contact is 6, 4, 4 and 2 for Pt–Ag, Pt–Cu, Pd–Ag and Pd–Cu 3:2 mixed-metal complexes with discrete structures, respectively; the M–M' distances in the platinum compounds are shorter than those in the palladium; the deviation of M from the surrounding four S atoms in the $M(S_2CNR_2)_2$ unit of the Pt–M' compounds is greater than that in the Pd–M' compounds and also in the M–Ag compounds than in the M–Cu compounds. These observations indicate that there is a strong M–M' bonding interaction in the Pt–Ag compounds and a weak one in compounds containing Pd and/or Cu. The $^{195}Pt-^{107,109}Ag$ coupling constant of 194 Hz observed for $[Pt_3(S_2CNBu^n_2)_6Ag_2]^{2+}$ supports the existence of a Pt–Ag bonding interaction. We have attempted to prepare similar 3:2 reaction products with other ligands such as alkyl dithiocarbonate, dithiolene and maleonitriledithiolate, but all attempts failed.

Acknowledgements

References

1 R. Uson, J. Fornies, M. Tomas, F. A. Cotton and L. R. Falvello, *J. Am. Chem. Soc.*, 1984, **106**, 2482; R. Uson, J. Fornies, B. Menjon, F. A. Cotton, L. R. Falvello and M. Tomas, *Inorg. Chem.*, 1985, **24**, 4651; R. Uson, J. Fornies, M. Tomas, J. M. Casas, F. A. Cotton and L. R. Falvello, *J. Am. Chem. Soc.*, 1985, **107**, 2556; R. Uson, J. Fornies, M. Tomas, J. M. Casas, F. A. Cotton and L. R. Falvello, *Inorg. Chem.*, 1986, **25**, 4519; R. Uson, J. Fornies, M. Tomas, J. M. Casas, F. A. Cotton and L. R. Falvello, *Polyhedron*, 1986, **5**, 901; F. A. Cotton, L. R. Falvello, R. Uson, J. Fornies, M. Tomas, J. M. Casas and I. Ara, *Inorg. Chem.*, 1987, **26**, 1366; R. Uson, J. Fornies, M. Tomas, I. Ara and J. M. Casas, *Inorg. Chem.*, 1989, **28**, 2388.

2 J. Fornies, R. Navarro, M. Tomas and E. Urriolabeitia, *Organometallics*, 1993, **12**, 940.

3 A. Albinati, S. Chaloupka, F. Demartin, T. F. Koetzle, H. Ruegger, L. M. Venanzi and M. K. Wolfer, *J. Am. Chem. Soc.*, 1993, **115**, 169.

4 A. Albinati, H. Lehner, L. M. Venanzi and M. Wolfer, *Inorg. Chem.*, 1987, **26**, 3933.

5 D. Coucouvanis, N. C. Baenzinger and S. M. Johnson, *Inorg. Chem.*, 1974, **13**, 1191; F. J. Hollander, Y. L. Ip and D. Coucouvanis, *Inorg. Chem.*, 1976, **15**, 2230.

6 L. M. Engelhardt, P. C. Healy, R. I. Papasergio and A. H. White, *Inorg. Chem.*, 1985, **24**, 382; L. M. Engelhardt, P. C. Healy, R. M. Shephard, B. W. Skelton and A. H. White, *Inorg. Chem.*, 1988, **27**, 2371; L. M. Engelhardt, P. C. Healy, B. W. Skelton and A. H. White, *Aust. J. Chem.*, 1988, **41**, 839; L. M. Engelhardt, P. C. Healy, B. W. Skelton and A. H. White, *Aust. J. Chem.*, 1989, **42**, 885; P. C. Healy, B. W. Skelton and A. H. White, *J. Chem. Soc.*, *Dalton Trans.*, 1989, 971.

7 J. A. McCleverty, S. McLuckie, N. J. Morrison, N. A. Bailey and N. W. Walker, *J. Chem. Soc.*, *Dalton Trans.*, 1977, 359.

8 R. M. Golding, A. D. Rae, B. J. Ralph and L. Sulligoi, *Inorg. Chem.*, 1974, **10**, 2499.

9 A. Z. Amanov, G. A. Kukina and M. A. Porai-Koshits, *Zh. Strukt. Khim.*, 1967, **8**, 174; M. Riekkola, T. Pakkanen and L. Ninisto, *Acta Chem. Scand.*, *Ser. A*, 1983, **37**, 807; A. T. Baker and M. T. Emett, *Aust. J. Chem.*, 1992, **45**, 429.

10 H. Yamaguchi, A. Kido and K. Yasukouchi, *Bull. Chem. Soc. Jpn.*, 1976, **49**, 1271; H. Anacker-Eickhoff, R. Hesse, P. Jennische and A. Wahlberg, *Acta Chem. Scand.*, *Ser. A*, 1982, **36**, 251.

11 R. Hesse and L. Nilson, *Acta Chem. Scand.*, 1969, **23**, 825.

12 R. Hesse, *Ark. Kemi*, 1962, **20**, 481.

13 A. M. Bond, R. Colton and D. R. Mann, *Inorg. Chem.*, 1989, **28**, 54.

14 A. M. Bond, R. Colton, J. C. Traeger and J. Harvey, *Inorg. Chim. Acta*, 1993, **212**, 233.

15 M. Ebihara, K. Sakurai, T. Kawamura, H. Katayama, H. Masuda and T. Taga, *Chem. Lett.*, 1990, 415.

16 M. Ebihara, K. Tokoro, K. Imaeda, K. Sakurai, H. Masuda and T. Kawamura, *J. Chem. Soc.*, *Chem. Commun.*, 1992, 1592.

17 T. Kawamura, M. Ebihara, K. Sakurai, S. Takahashi, H. Masuda and T. Taga, *Rep. Asahi Glass Found.*, 1991, **59**, 133.

18 A. M. Bond, R. Colton, Y. A. Mah and J. C. Traeger, *Inorg. Chem.*, 1994, **33**, 2548.

19 J. M. C. Alison and T. A. Stephenson, *J. Chem. Soc.*, *Dalton Trans.*, 1973, 254.

20 G. J. Kubas, *Inorg. Synth.*, 1979, **19**, 90.

21 D. T. Cromer and J. T. Waber, in *International Tables for X-Ray Crystallography*, Kynoch Press, Birmingham, 1974, vol. 4.

22 D. C. Creagh and W. J. McAuley, in *International Tables for X-Ray Crystallography*, ed. A. J. C. Wilson, Kluwer Academic Publishers, Boston, 1992, vol. C, pp. 219–222.

23 N. Walker and D. Stuart, *Acta Crystallogr.*, *Sect. A*, 1983, **39**, 158.

24 G. M. Sheldrick, in *Crystallographic Computing 3*, eds. G. M. Sheldrick, C. Kruger and R. Goddard, Oxford University Press, 1985, pp. 175–189.

25 S. J. La Placa and J. A. Ibers, *Acta Crystallogr.*, 1965, **18**, 511.

26 A. C. T. North, D. C. Phillips and F. S. Mathews, *Acta Crystallogr. Sect. A*, 1968, **24**, 351.

27 G. J. Gilmore, *J. Appl. Crystallogr.*, 1984, **17**, 42.

28 R. P. F. Kanters, P. P. J. Schlebos, J. J. Bour, W. P. Bosman, J. M. M. Smits, P. T. Beurskens and J. J. Steggerda, *Inorg. Chem.*, 1990, **29**, 324.

29 M. F. J. Schoondergang, J. J. Bour, P. P. J. Schlebos, A. W. P. Vermeer, W. P. Bosman, J. M. M. Smits, P. T. Beurskens and J. J. Steggerda *Inorg. Chem.*, 1991, **30**, 4704.

30 A. Albinati, K.-H. Dahmen, A. Togni and L. M. Venanzi, *Angew. Chem.*, *Int. Ed. Engl.*, 1985, **24**, 766.

31 G. L. Arsenault, C. M. Anderson and R. J. Puddephatt, *Organometallics*, 1988, **7**, 2094.

32 A. F. M. J. van der Ploeg, G. van Koten and C. Brevard, *Inorg. Chem.*, 1982, **21**, 2878.